

Role of Hetero-Halogen ($F \cdots X$, $X = Cl, Br$, and I) or Homo-Halogen ($X \cdots X$, $X = F, Cl, Br$, and I) Interactions in Substituted Benzanilides

Published as part of a virtual special issue on Structural Chemistry in India: Emerging Themes.

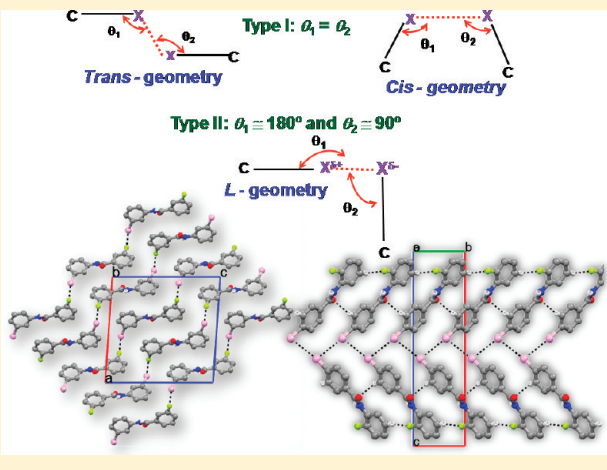
Susanta K. Nayak,[†] M. Kishore Reddy,[†] Tayur N. Guru Row,^{*,†} and Deepak Chopra^{*,†}

[†]Solid State and Structural Chemistry Unit, Indian Institute of Science, Bangalore 560012, Karnataka, India

[‡]Department of Chemistry, Indian Institute of Science Education and Research, ITI (Gas Rahat Building), Govindpura, Bhopal 462023

 Supporting Information

ABSTRACT: A series of halogen-substituted benzanilides have been synthesized and characterized, and crystallization studies directed toward generation of polymorphs have been performed to delineate the importance of interactions involving halogens. The effect of halogen substitution on the molecular conformation and supramolecular packing has been investigated. The $N-H \cdots O$ H-bond is a key structure-directing element acting in conjunction with $C-H \cdots O$ and $C-H \cdots \pi$ interactions. In addition, it is of importance to note that organic fluorine prefers Type I $F \cdots F$ contacts, whereas Cl, Br , and I prefer Type II contacts. Hetero-halogen \cdots halogen interactions on the other hand are predominately of Type II geometry, and this is due to the greater polarizability of the electron density associated with the heavier halogens. It is of importance to evaluate the contributing role of these interactions in crystal structure packing and the co-operativity associated with such interactions in the solid state.



INTRODUCTION

Halogenated compounds, in particular, fluorinated molecules, have received considerable attention in chemistry and biology.¹ Introduction of fluorine (15% of all pharmaceuticals include at least one fluorine atom²) into biologically active compounds results in improved pharmacological properties. The physical and chemical properties of compounds are altered by replacing the hydrogen atoms with fluorine, due to its high electronegativity, low polarizability, and bond strength.³ Though the role of fluorine involved interactions ($C-H \cdots F$, $F \cdots F$, $C-F \cdots \pi$) are considered weak, it plays a vital role in directing the molecular assembly which has been highlighted by Hülliger and co-workers and several other research groups.⁴ The importance of $C-H \cdots F$ interactions in the absence of strong hydrogen bonds has been well established.⁵ The evaluation of weak interactions in the presence of strong hydrogen bonds has generated widespread interest among the crystal engineering community, particularly with the design and application of these compounds in the area of polymorphism. Recent efforts have been directed toward the understanding of intra- and intermolecular interactions involving “ordered” and “disordered” organic fluorine in tetrahydroindoles and mono- and di-fluorinated benzanilides.⁶

Benzanilides are present in a wide range of biological compounds and serve as intermediates for many pharmaceutical compounds.⁷ Differently substituted benzanilides have been used as

CCRS receptor ligands, anti-inflammatory, antiviral agents, and in the application of voltage-dependent potassium channel operators.⁸ This molecular system allows one to explore the regime of strong $N-H \cdots O$ hydrogen bonds (presence of amino and carbonyl group), weak $C-H \cdots O$ hydrogen bonds (activated $C-H$), weak $N-H \cdots F$ (intra)/ $C-H \cdots F/F \cdots F$ (presence of organic fluorine on either or both aromatic rings), and finally the weakest of all intermolecular interactions, which includes $C-H \cdots \pi$ and $\pi \cdots \pi$ interactions. Subtle differences in the energetics associated with weak and flexible $C-H \cdots F$ interactions have resulted in the formation of polymorphs⁹ and in situ cryocrystallization of liquids.¹⁰ Topological characterization of weak $C-H \cdots F$ and $C-F \cdots F-C$ contacts using high resolution charge density data have also been performed.¹¹ The significance of intramolecular $N-H \cdots F$ hydrogen bonds has been utilized for the construction of folding architectures in aromatic amides.¹² Again the preference of an intramolecular six-/five-membered $N-H \cdots X$ ($X = Cl, Br$, and I) hydrogen bonding pattern in the absence or presence of intermolecular $N-H \cdots O$ hydrogen bonds has been highlighted in halogenated aromatic amides.^{13,14}

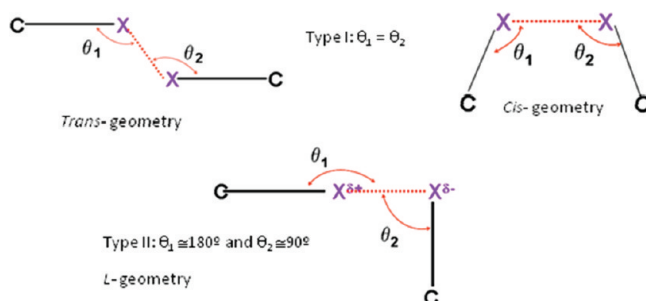
In view of the above-mentioned interests, it was of interest to explore the nature of intermolecular interactions in halogenated benzanilides, containing bromine, chlorine, and iodine in the

Received: November 21, 2010

Revised: January 16, 2011

Published: March 14, 2011

Scheme 1. Geometrical Classification of Halogen···Halogen Interaction as Type I and Type II



presence of organic fluorine and to illustrate the changes in supramolecular assembly [the importance of homo (symmetric) $X\cdots X$ (F, Cl, Br, and I), $X\cdots Y$ (F, Cl, Br, and I), hetero (unsymmetrical) halogen, and $C-X\cdots \pi$ (F, Cl, Br, and I) interactions] which govern crystal formation.^{15,16} The evaluation of homo (symmetric) interactions has been performed on a series of benzanilides, containing the halogen chlorine on either or both of the aromatic phenyl rings.¹⁷ Such halogen–halogen interactions have been termed as Type I (*cis* and *trans* geometry) and Type II (electrophile-nucleophile model) depending on the angular approach of the halogens toward each other (Scheme 1). These have been coined “attractive” in an investigation performed on $\text{CH}_3/\text{H}-\text{F}\cdots \text{Cl}-\text{CF}_3$ dimers via a decomposition of the interaction energy. The presence of a trifluoromethyl group linked to chlorine leads to an enhanced polarization of the C–Cl bond resulting in an increased strength of the $\text{Cl}\cdots \text{F}$ contact.¹⁸ Recently, the application of Voronoi–Dirichlet polyhedrals (VDPs) has been demonstrated to analyze intermolecular interactions in crystal structures of halogens or interhalogen compounds to understand structure–property correlations in this class of molecules.¹⁹

We present here the importance of fluorine in the presence of other halogen (Cl, Br, or I) atoms in dihalogenated benzanilide compounds to evaluate the preference of hetero-halogen $\text{F}\cdots \text{X}$ (Cl, Br, and I) over homo-halogen $\text{X}\cdots \text{X}$ (F, Cl, Br, and I) interactions along with other weak ($\text{C}-\text{H}\cdots \text{F}/\text{Cl}/\text{Br}$, $\text{C}-\text{X}\cdots \pi$) and strong ($\text{N}-\text{H}\cdots \text{O}$) hydrogen bonds. In this context, we have synthesized several possible combinations of such compounds having a single fluorine atom on one of the aromatic rings while the other ring has a different halogen (Cl, Br, or I) substitution (Figure 1).

It is important to describe the nomenclature used in this article at this stage since a large number of compounds have been studied. In this context, Table 1 gives the details of abbreviations used for naming the compounds as shown in Figure 2.

■ EXPERIMENTAL SECTION

Synthesis and Crystallization. The dihalogenated benzanilides were prepared by the reaction of mono halogen substituted aniline (*ortho*, *meta*, *para*) (2.626 mmol) and 4-diaminomethylaminopyridine (2.626 mmol) in dry dichloromethane in a nitrogen atmosphere as mentioned in Figure 1.²¹ Respectively, a mono halogenated benzoyl chloride (*ortho*, *meta*, *para*) (2.626 mmol) was added dropwise with stirring at room temperature. The mixture was stirred for 12 h at room temperature. The reaction progress was monitored by thin layer chromatography. The solvent was removed in vacuo and solid was extracted with DCM solvent. The infrared (IR) value for amide

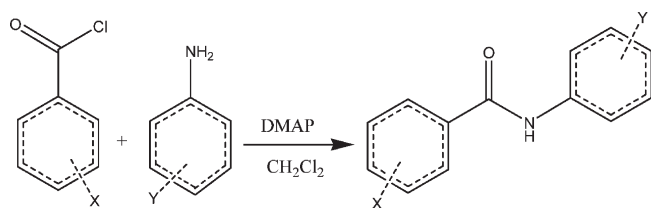


Figure 1. Synthetic procedure of dihalogenated benzanilides (all combination of mixed halogen keeping fluorine in one side of the ring): When X = F [*ortho* (2), *meta* (3), *para* (4)]; Y = Cl or Br or I [*ortho* (2), *meta* (3), *para* (4)]; Y = F [*ortho* (2), *meta* (3), *para* (4)].

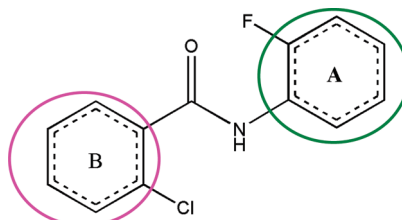


Figure 2. Representation of the nomenclature used in this chapter. Circles are drawn to identify the two sides: Aniline side (A) and benzoyl side (B). (For example: 2FA-2CIB represents the compound in Group 1; Set 1.)

($\text{C}=\text{O})\nu_{\text{max}} = 1650 \text{ cm}^{-1}$ provides the evidence for the product formation. Further, the purity of sample was characterized by melting point, NMR, and powder X-ray data. Single crystals of desired size and quality were grown by slow evaporation at 0 and 25 °C by dissolving the substance in different solvent combinations such as (ethyl acetate/hexane) and (dichloromethane/hexane). Morphologies ranging from thin plates to fibrous needles were obtained.

Single Crystal Data Collection and Refinement. Single crystal X-ray diffraction data of some of these compounds were collected on a Bruker AXS SMART APEX CCD diffractometer with X-ray generator operating at 50 kV and 35 mA using graphite monochromated MoK_{α} ($\lambda = 0.7107 \text{ \AA}$)²² radiation. The data for rest of the compounds were recollected on CrysAlis CCD Xcalibur, Eos (Nova), Oxford Diffraction with X-ray generator operating at 50 kV and 1 mA, using MoK_{α} radiation ($\lambda = 0.7107 \text{ \AA}$).²³ Data were collected for 606 frames per set by using SMART with different settings of φ (0°, 90°, 180°) keeping a sample to detector distance of 6.062 cm and the 2θ value fixed at -25° . Data reduction and analysis were performed by SAINTPLUS, XPREP, and SADABS.²⁴ The structures were solved and refined by using SHELXL97,²⁴ using the program suite WinGX.²⁵ The molecular diagrams were generated using ORTEP-3,²⁶ and the packing diagrams were generated using Mercury.²⁷ The geometric calculations were carried out by PARST95²⁸ and PLATON.²⁹ The non-hydrogen atoms are refined anisotropically and the hydrogen atoms bonded to C and N atoms were positioned geometrically and refined using a riding model with distance restraints of $\text{N}-\text{H} = 0.86 \text{ \AA}$, aromatic $\text{C}-\text{H} = 0.93 \text{ \AA}$ and with $U_{\text{iso}}(\text{H}) = 1.2U_{\text{eq}}(\text{N},\text{C})$. Tables 2, 5, 8, 11, 13 and 16. lists all crystallographic details. Intra- and intermolecular interactions are listed in Tables 3, 6, 9, 12, 14 and 17. whereas halogen···halogen interactions are listed in Tables 4, 7, 10, 15 and 18. ORTEP plots and dihedral angles are included in Supporting Information (Figure S1 and Table S1).

■ RESULTS

Group A (Set I). 2FA-2CIB crystallizes in the centrosymmetric monoclinic space group $P2_1/n$ with $Z = 4$ (Figure 3a, Table 2). It is noteworthy that all the crystal structures discussed

Table 1. Description of Abbreviations Used for the Compounds Studied in this Section

		fluorine on the aniline side (A) IUPAC nomenclature	remark
Group A			
Set I	2FA-2ClB	2-chloro-N-(2-fluorophenyl)benzamide	
	2FA-2BrB	2-bromo-N-(2-fluorophenyl)benzamide	
	2FA-2IB	2-iodo-N-(2-fluorophenyl)benzamide	
Set II	2FA-3ClB	3-chloro-N-(2-fluorophenyl)benzamide	quality crystals not obtained ^a
	2FA-3BrB	3-bromo-N-(2-fluorophenyl)benzamide	b
	2FA-3IB	3-iodo-N-(2-fluorophenyl)benzamide	
Set III	2FA-4ClB	4-chloro-N-(2-fluorophenyl)benzamide	quality crystals not obtained ^a
	2FA-4BrB	4-bromo-N-(2-fluorophenyl)benzamide	
	2FA-4IB	4-iodo-N-(2-fluorophenyl)benzamide	
Group B			
Set I	3FA-2ClB	2-chloro-N-(3-fluorophenyl)benzamide	disorder
	3FA-2BrB	2-bromo-N-(3-fluorophenyl)benzamide	disorder
	3FA-2IB	2-iodo-N-(3-fluorophenyl)benzamide	disorder
Set II	3FA-3ClB	3-chloro-N-(3-fluorophenyl)benzamide	quality crystals not obtained ^a
	3FA-3BrB	3-bromo-N-(3-fluorophenyl)benzamide	disorder
	3FA-3IB	3-iodo-N-(3-fluorophenyl)benzamide	quality crystals not obtained ^a
Set III	3FA-4ClB	4-chloro-N-(3-fluorophenyl)benzamide	
	3FA-4BrB	4-bromo-N-(3-fluorophenyl)benzamide	
	3FA-4IB	4-iodo-N-(3-fluorophenyl)benzamide	quality crystals not obtained ^a
Group C			
Set I	4FA-2ClB	2-chloro-N-(4-fluorophenyl)benzamide	
	4FA-2BrB	2-bromo-N-(4-fluorophenyl)benzamide	
	4FA-2IB	2-iodo-N-(4-fluorophenyl)benzamide	quality crystals not obtained ^a
Set II	4FA-3ClB	3-chloro-N-(4-fluorophenyl)benzamide	
	4FA-3BrB	3-bromo-N-(4-fluorophenyl)benzamide	
	4FA-3IB	3-iodo-N-(4-fluorophenyl)benzamide	quality crystals not obtained ^a
Set III	4FA-4ClB	4-chloro-N-(4-fluorophenyl)benzamide	quality crystals not obtained ^a
	4FA-4BrB	4-bromo-N-(4-fluorophenyl)benzamide	
	4FA-4IB	4-iodo-N-(4-fluorophenyl)benzamide	quality crystals not obtained ^a
fluorine on the benzoyl side (B) IUPAC nomenclature			
Group D			
Set I	2FB-2ClA	2-fluoro-N-(2-chlorophenyl)benzamide	disorder
	2FB-2BrA	2-fluoro-N-(2-bromophenyl)benzamide	disorder
	2FB-2IA	2-fluoro-N-(2-iodophenyl)benzamide	disorder
Set II	2FB-3ClA	2-fluoro-N-(3-chlorophenyl)benzamide	
	2FB-3BrA	2-fluoro-N-(3-bromophenyl)benzamide	
	2FB-3IA	2-fluoro-N-(3-iodophenyl)benzamide	quality crystals not obtained ^a
Set III	2FB-4ClA	2-fluoro-N-(4-chlorophenyl)benzamide	quality crystals not obtained ^a
	2FB-4BrA	2-fluoro-N-(4-bromophenyl)benzamide	
	2FB-4IA	2-fluoro-N-(4-iodophenyl)benzamide	quality crystals not obtained ^a
Group E			
Set I	3FB-2ClA	3-fluoro-N-(2-chlorophenyl)benzamide	
	3FB-2BrA	3-fluoro-N-(2-bromophenyl)benzamide	
	3FB-2IA	3-fluoro-N-(2-iodophenyl)benzamide	quality crystals not obtained ^a
Set II	3FB-3ClA	3-fluoro-N-(3-chlorophenyl)benzamide	
	3FB-3BrA	3-fluoro-N-(3-bromophenyl)benzamide	
	3FB-3IA	3-fluoro-N-(3-iodophenyl)benzamide	quality crystals not obtained ^a
Set III	3FB-4ClA	3-fluoro-N-(4-chlorophenyl)benzamide	disorder
	3FB-4BrA	3-fluoro-N-(4-bromophenyl)benzamide	disorder

Table 1. Continued

			fluorine on the benzoyl side (B) IUPAC nomenclature	
	3FB-4IA		3-fluoro-N-(4-iodophenyl)benzamide	quality crystals not obtained ^a
			Group F	
Set I	4FB-2ClA		4-fluoro-N-(2-chlorophenyl)benzamide	
	4FB-2BrA		4-fluoro-N-(2-bromophenyl)benzamide	
	4FB-2IA		4-fluoro-N-(2-iodophenyl)benzamide	
Set II	4FB-3ClA		4-fluoro-N-(3-chlorophenyl)benzamide	
	4FB-3BrA		4-fluoro-N-(3-bromophenyl)benzamide	
	4FB-3IA		4-fluoro-N-(3-iodophenyl)benzamide	
Set III	4FB-4ClA		4-fluoro-N-(4-chlorophenyl)benzamide	
	4FB-4BrA		4-fluoro-N-(4-bromophenyl)benzamide	
	4FB-4IA		4-fluoro-N-(4-iodophenyl)benzamide	quality crystals not obtained ^a

^a Crystals were obtained for such compounds. However, these are not suitable enough for single crystal XRD. Crystallization experiments are still currently underway which are directed toward obtaining quality crystals for crystal structure determination.^b This structure exhibits polymorphic behavior and disorder structures are reported in a private communication.²⁰ However, it may be mentioned that one of the polymorphs is isostructural to 2FA-3BrB.

Table 2. Crystallographic Information

	Set (I)		Set (II)		Set (III)		
	2FA-2ClB	2FA-2BrB	2FA-3ClB ^a	2FA-3BrB	2FA-4ClB	2FA-4BrB	2FA-4IB
formula	C ₁₃ H ₉ NOFCl	C ₁₃ H ₉ NOFBr	C ₁₃ H ₉ NOFCl	C ₁₃ H ₉ NOFBr	C ₁₃ H ₉ NOFCl	C ₁₃ H ₉ NOFBr	C ₁₃ H ₉ NOFI
formula weight	249.7	294.1	249.7	294.1	249.7	294.1	341.1
temperature K	292(2)	292(2)	292(2)	292(2)	292(2)	292(2)	292(2)
size of crystal (mm)	0.30 × 0.28 × 0.21	0.34 × 0.22 × 0.12	0.24 × 0.22 × 0.15	0.27 × 0.05 × 0.04	0.28 × 0.21 × 0.19	0.30 × 0.23 × 0.15	0.23 × 0.16 × 0.14
CCDC no.	774783	765329	751294	765330	774786	765331	774780
space group	P2 ₁ /n	Pna2 ₁	P2 ₁ /c	P2 ₁ /c	P2 ₁	P2 ₁	P2 ₁
<i>a</i> (Å)	4.912 (1)	12.410(2)	23.905(5)	23.935(2)	4.918(5)	4.919(1)	4.919(3)
<i>b</i> (Å)	5.858(2)	11.071(2)	4.996(1)	4.966(1)	5.597(5)	5.616(1)	5.577(3)
<i>c</i> (Å)	39.459(5)	8.605(1)	19.392(4)	19.884(2)	20.553(5)	21.009(5)	21.819(1)
α (°)	90	90	90	90	90	90	90
β (°)	90.362(2)	90	101.290(4)	102.297(2)	90.128(5)	90.115(28)	91.038(6)
γ (°)	90	90	90	90	90	90	90
volume (Å ³)	1135.4(1)	1182.3(1)	2271.0(2)	2309.4(1)	565.7(5)	580.4(2)	598.5(2)
<i>Z</i>	4	4	8	8	2	2	2
density (g cm ⁻³)	1.46	1.65	1.46	1.69	1.47	1.68	1.89
μ (mm ⁻¹)	0.330	3.471	0.330	3.554	0.331	3.535	2.670
<i>F</i> (000)	511.9	583.9	1023.9	1167.8	256.0	292.0	328
θ _{min, max} (°)	2.1, 26.0	2.5, 28.0	1.7, 25.0	1.7, 26.0	3.8, 26.0	1.9, 26.0	2.8, 26.0
<i>h</i> _{min, max}	−6, 6	−16, 15	−28, 28	−29, 29	−6, 6	−6, 6	−6, 6
<i>k</i> _{min, max}	−7, 6	−14, 13	−5, 5	−5, 6	−6, 6	−6, 6	−6, 6
<i>l</i> _{min, max}	−48, 48	−11, 11	−23, 23	−24, 22	−25, 25	−25, 24	−26, 26
no. of reflections measured	8265	9784	20215	16710	6357	4434	6486
no. unique reflections	2229	2797	3983	4508	1337	2226	2324
no. of parameter	154	158	307	307	154	154	155
R _{all} , R _{obs}	0.100, 0.073	0.052, 0.035	0.177, 0.064	0.093, 0.044	0.072, 0.036	0.060, 0.039	0.077, 0.073
wR _{2_all} , wR _{2_obs}	0.146, 0.139	0.083, 0.077	0.109, 0.089	0.085, 0.077	0.075, 0.066	0.081, 0.075	0.205, 0.203
Δρ _{max, min} (e Å ⁻³)	0.292, −0.252	0.532, −0.477	0.213, −0.187	0.458, −0.272	0.121, −0.138	0.655, −0.188	2.350, −1.705
GOF	1.158	1.011	0.898	0.941	0.832	1.004	1.141

^a Exhibit polymorphism.²⁰

in this chapter exhibit the N—H···O hydrogen bond chains as a common feature (Figure 3b). In addition, a dimeric motif involving C—H···F and C—H···Cl provides stability to the crystal packing by forming a two-dimensional (2-D) network as

shown in Figure 3c (Table 3). 2FA-2BrB is not isostructural and crystallizes in noncentrosymmetric orthorhombic space group Pna2₁ (*Z* = 4). An intramolecular C—H···O bond stabilizes the conformation of the molecule (Figure 4a). In addition to

Table 3. Intra- and Intermolecular Interactions^a

	D–H···A	D···H/Å	D···A/Å	H···A/Å	∠D–H···A/°	symmetry
2FA-2ClB	N1–H1···O1	0.86	2.869(3)	2.02	168	$1 + x, y, z$
	C12–H12···F1	0.93	3.587(5)	2.67	168	$x - 1, +y - 1, +z$
	C10–H10···F1	0.93	3.437(5)	2.70	136	$-x + 1/2 + 2, y - 1/2, -z + 1/2$
	C3–H3···Cl1	0.93	3.642(4)	2.97	130	$x - 1, y - 1, z$
2FA-2BrB	C13–H13···O1	0.93	2.907(4)	2.42	113	x, y, z
	N1–H1···O1	0.68(3)	2.945(3)	2.27	169	$-x, 1 - y, -1/2 + z$
	C10–H10···O1	0.93	3.438(5)	2.52	170	$1/2 - x, -1/2 + y, -1/2 + z$
	C4–H4···Br1	0.93	3.776(4)	3.03	137	$x + 1/2 + 2, -y + 1/2, z$
2FA-3BrB	C13–H13···O1	0.93	2.919(4)	2.46	111	x, y, z
	C13'–H13'···O1'	0.93	2.934(4)	2.48	110	x, y, z
	N1–H1···O1	0.86	2.927(4)	2.12	156	$x, -1 + y, z$
	N1'–H1'···O1'	0.86	2.894(4)	2.09	155	$x, 1 + y, z$
	C2–H2···F1'	0.93	3.257(4)	2.50	139	$x, -1 + y, z$
	C10'–H10'···F1	0.93	3.380(4)	2.46	173	$x, 1 + y, z$
	C13–H13···Cg4	0.93	3.753(4)	2.98	148	x, y, z
	C13–H13···O2	0.93	2.907(5)	2.45	110	x, y, z
2FA-4ClB	N1–H1···O2	0.86	2.937(4)	2.13	156	$-1 + x, y, z$
	C12–H12···F1	0.93	3.414(5)	2.50	169	$1 + x, 1 + y, z$
	C3–H3···O1	0.93	3.454(4)	2.59	154	$1 + x, -1 + y, z$
	C13–H13···O1	0.93	2.899(4)	2.44	111	x, y, z
2FA-4BrB	N1–H1···O1	0.86	2.942(3)	2.14	155	$1 + x, y, z$
	C12–H12···F1	0.93	3.414(4)	2.50	169	$-1 + x, 1 + y, z$
	C3–H3···O1	0.93	3.470(5)	2.63	153	$x - 1, y - 1, z$
	C13–H13···O1	0.93	2.95(2)	2.48	111	x, y, z
2FA-4IB	N1–H1···O1	0.86	2.915(13)	2.11	155	$-1 + x, y, z$
	C12–H12···F1	0.93	3.400(18)	2.49	166	$1 + x, 1 + y, z$
	C3–H3···O1	0.93	3.540(3)	2.69	151	$x + 1, y - 1, z$

^a Cg4 = centroid of C5'–C13' atom.

Table 4. Halogen···Halogen Short Contact

	C–X···Y–C	X···Y/Å	∠C–X···Y/°	∠C–Y···X/°	symmetry	type
2FA-3BrB	C5–Br1···Br1'–C5'	3.721(3)	172	110	$-x, -y + 2, -z + 1$	II
2FA-4ClB	C4–Cl1···Cl1–C4	3.548(1)	171	92	$-x + 1, +y - 1/2, -z + 1$	II
2FA-4BrB	C4–Br1···Br1–C4	3.656(2)	172	86	$-x, +y - 1/2, -z + 1$	II
2FA-4IB	C4–I1···I1–C4	3.873(1)	93	174	$-x + 1, y - 1/2, -z + 1$	II

N–H···O intermolecular hydrogen bond, C–H···O and C–H···Br contacts result in the formation a “wavelike” packing feature along the *a*-axis (Figure 4b and Table 3).

Group A (Set II). 2FA-3ClB and 2FA-3BrB are isostructural and crystallize in a monoclinic space group *P2*₁/*c* with *Z* = 8 (*Z'* = 2) (Table 2). Indeed, 2FA-3ClB exhibits polymorphism.²⁰ Intramolecular C–H···O (involving H13) interaction stabilizes the molecular conformation. In addition to the strong N–H···O hydrogen bond, the two independent molecules are held together by a C–H···π interaction (Table 3). This also induces the formation of a C–H···F dimer motif across the crystallographic 2-fold symmetry (Figure 5). It is interesting to note that while a Type I, Cl···Cl short contact [3.33 Å, $\theta_1 \approx \theta_2 \approx 165^\circ$] is observed in 2FA-3ClB, a Type II, Br···Br contact [3.72 Å, $\theta_1 = 172$, $\theta_2 = 110^\circ$] (sum of van der Waals radii +0.1 Å) is observed in 2FA-3Br. This rather unusual feature could be attributed to the size of bromine, and a detailed charge density analysis could bring out the finer

details of the polarizability versus size factor in halogen···halogen interaction (Table 4).

Group A (Set III). 2FA-4ClB, 2FA-4BrB, and 2FA-4IB are isostructural with noncentrosymmetric monoclinic *P2*₁ space group with *Z* = 2 (Table 2). All the three structures show the intramolecular C–H···O interaction involving H13 which lock the molecular conformation. N–H···O hydrogen bonds form chains along the *a*-axis which are further stabilized by additional C–H···O (involving H3) and C–H···F (involving H12) weak interactions (Table 3). The C–H···O and C–H···F interactions form a dimer motif arrangement. Homo-halogen X···X (Cl, Br, and I) interactions of Type II [$\theta_1 \approx 172$, $\theta_2 \approx 86$ –110°] are preferred which generate a zigzag chain along with the C–H···O and C–H···F chains (Figure 6, Table 4).

Group B (Set I and Set II). Compounds belonging to Group B set I and II are either disordered²⁰ or do not yield X-ray diffraction quality crystals.

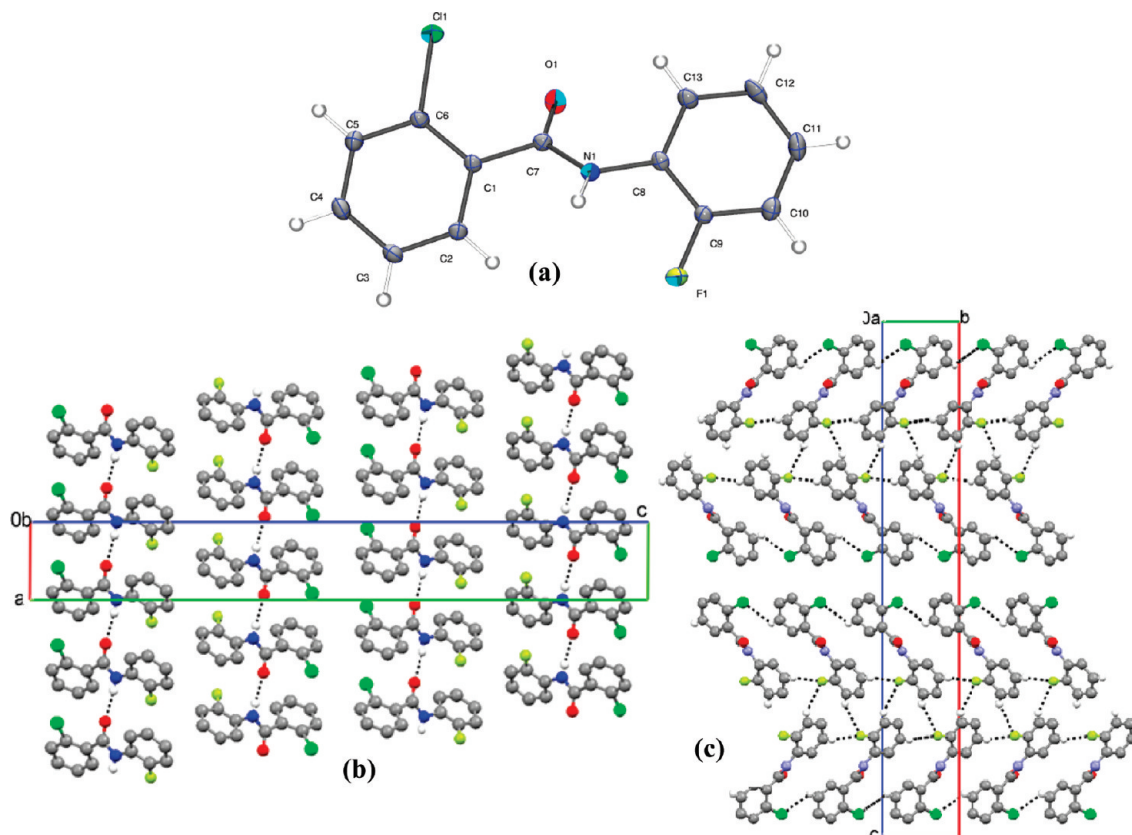


Figure 3. (a) ORTEP of 2FA-2ClB with 30% ellipsoid probability and atom numbering scheme (b) N–H \cdots O hydrogen bond chains along the *a*-axis (c) C–H \cdots F and C–H \cdots Cl interactions forming chains and dimer.

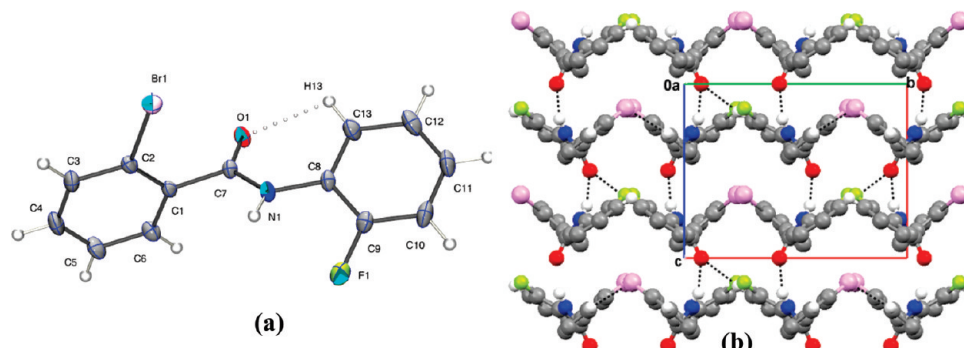


Figure 4. (a) ORTEP of 2FA-2BrB with 30% ellipsoid probability, atom numbering scheme, and intramolecular interaction depicted by open circles, (b) N–H \cdots O hydrogen bond chains, C–H \cdots O and C–H \cdots Br interactions forming a wavelike pattern.

Group B (Set III). 3FA-4ClB and 3FA-4BrB are isostructural and crystallize in the non-centrosymmetric orthorhombic space group $P2_12_12_1$ with $Z = 4$ (Table 5). Intramolecular C–H \cdots O interaction (involving H13) stabilizes the molecular conformation. N–H \cdots O hydrogen bonds form molecular chain along the *a*-axis. Further, the molecular packing is stabilized by C–H \cdots O (involving H3) and C–H \cdots F (involving H9) interactions also along the *a*-axis (Table 6). Additional homo-halogen X \cdots X (Cl, Br) of Type II geometry contacts [$\theta_1 \approx 172$, $\theta_2 \approx 84^\circ$] link the N–H \cdots O chains (Figure 7, Table 7).

Group C (Set I). 4FA-2ClB and 4FA-2BrB are again isostructural and crystallize in centrosymmetric triclinic space group $P\bar{1}$ with $Z = 2$ (Table 8). An intramolecular C–H \cdots O hydrogen

bond involving H13 stabilizes the molecular conformation. The N–H \cdots O hydrogen bonds form chains along the *a*-axis, and further weak C–H \cdots F interactions (involving H5) form molecular chains along the *c*-axis provide additional stability (Table 9). This set provides the hetero-halogen F \cdots X (Cl or Br) [Type II, contacts are 3.189(4) and 3.160(2) Å for 4FA-2ClB and 4FA-2BrB respectively and angles are $\theta_1 \approx 178$ and $\theta_2 \approx 108^\circ$] interactions in this series of compounds to form layered structures with tetramer unit formation (Figure 8, Table 10).

Group C (Set II). 4FA-3ClB and 4FA-3BrB are isostructural with centrosymmetric monoclinic $P2_1/c$ space group with $Z = 4$ (Table 8). An intramolecular C–H \cdots O bond involving H13 once again stabilizes the molecular conformation. The N–H \cdots O

Table 5. Crystallographic Information

	3FA-4ClB	3FA-4BrB
formula	C ₁₃ H ₉ NOFCl	C ₁₃ H ₉ NOFBr
formula weight	249.7	294.1
temperature K	292(2)	292(2)
size of crystal (mm)	0.32 × 0.19 × 0.12	0.18 × 0.16 × 0.11
CCDC no.	774787	765332
space group	P2 ₁ 2 ₁ 2 ₁	P2 ₁ 2 ₁ 2 ₁
a (Å)	4.941(4)	4.931(1)
b (Å)	5.645(5)	5.671(1)
c (Å)	40.123(3)	40.929(7)
α (°)	90	90
β (°)	90	90
γ (°)	90	90
volume (Å ³)	1119.2(2)	1144.7(2)
Z	4	4
density (g cm ⁻³)	1.48	1.71
μ (mm ⁻¹)	0.335	3.585
F(000)	511.9	583.9
θ _{min} , max (°)	2.0, 26.0	2.0, 25.5
h _{min} , max	-6, 6	-5, 5
k _{min} , max	-6, 6	-6, 6
l _{min} , max	-49, 49	-49, 49
no. of reflections measured	11560	8452
no. unique reflections	2182	2104
no. of parameter	154	154
R _{all} , R _{obs}	0.079, 0.068	0.075, 0.057
wR ₂ _{all} , wR ₂ _{obs}	0.148, 0.144	0.122, 0.117
Δρ _{max} , min (e Å ⁻³)	0.458, -0.209	0.627, -0.366
GOF	1.209	1.152

hydrogen bond forms a molecular chain along the *b*-axis (Table 9, Figure 9a). It is to be noted that stability in packing is achieved through C—H···π interactions (Figure 9b). Despite the increased distances with respect to homo-halogen interaction, the geometry is maintained as Type I for fluorine [$\theta_1 = \theta_2 \approx 110^\circ$] and Type II for chlorine or bromine [$\theta_1 \approx 163$ and $\theta_2 \approx 97^\circ$] (Table 10, Figure 9b).

Group C (Set III). 4FA-4BrB crystallizes in centrosymmetric monoclinic space group P2₁/c with Z = 4 (Table 8). 4FA-4BrB is nearly isostructural to the parameters, being 1.0 Å larger in the *a*-axis and 5.9° lower in *β* angle compared to the lattice parameters for 4FA-3ClB. As a consequence, the packing of molecules in the crystal structure is similar to that of 4FA-3BrB. It is of interest to note that the shift in bromine position from meta to para on the benzoyl ring do not appear to be of any significance (Table 10 and Figure 9).

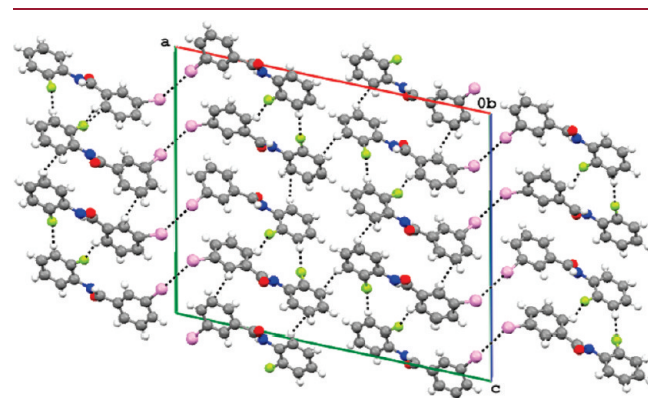


Figure 5. N—H···O, C—H···F (dimer) hydrogen bond chains and X···X (Cl and Br) interactions along with C—H···π form two differed layered structures for 2FA-3BrB and 2FA-3ClB.

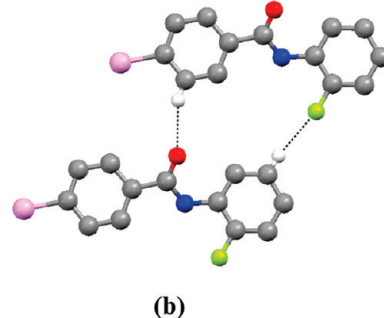
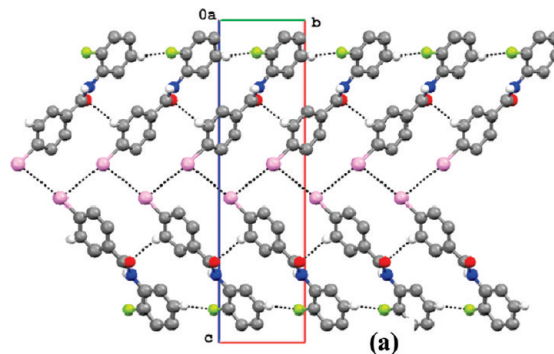


Figure 6. 2FA-4ClB, 2FA-4BrB, and 2FA-4IB depicting (a) homo-halogen X···X (Cl, Br, and I) zigzag chain parallel to C—H···F chains stabilized by C—H···O interaction (b) C—H···O and C—H···F exhibit dimer formation.

Table 6. Intra- and Intermolecular Interactions

crystal	D—H···A	D···H/Å	D···A/Å	H···A/Å	∠D—H···A/°	symmetry
3FA-4ClB	C13—H13···O1	0.93	2.865(5)	2.36	113	x, y, z
	N1—H1···O1	0.86	2.976(4)	2.19	151	-1 + x, y, z
	C3—H3···O1	0.93	3.438(5)	2.57	156	-1 + x, 1 + y, z
	C9—H9···F1	0.93	3.447(5)	2.54	167	-1 + x, 1 + y, z
3FA-4BrB	C13—H13···O1	0.93	2.868(8)	2.37	114	x, y, z
	N1—H1···O1	0.86	2.969(6)	2.19	151	-1 + x, y, z
	C3—H3···O1	0.93	3.442(8)	2.57	156	-1 + x, y, z
	C9—H9···F1	0.93	3.454(8)	2.54	166	-1 + x, y, z

Table 7. Halogen···Halogen Short Contact

crystal	C—X···Y—C	X···Y/Å	∠C—X···Y/°	∠C—Y···X/°	symmetry	type
3FA-4ClB	C4—Cl1···Cl1—C4	3.553(2)	171	83	$-x, y - 1/2, -z + 1/2$	II
3FA-4BrB	C4—Br1···Br1—C4	3.657(2)	172	85	$-x, y - 1/2, -z + 1/2$	II

Table 8. Crystallographic Information

	Set (I)		Set (II)		Set (III)	
	4FA-2ClB	4FA-2BrB	4FA-3ClB	4FA-3BrB	4FA-4BrB	
formula	C ₁₃ H ₉ NOFCl	C ₁₃ H ₉ NOFBr	C ₁₃ H ₉ NOFCl	C ₁₃ H ₉ NOFBr	C ₁₃ H ₉ NOFBr	
formula weight	249.7	294.1	249.7	294.1	294.1	
temperature K	292(2)	292(2)	292(2)	292(2)	292(2)	
size of crystal (mm)	0.24 × 0.22 × 0.19	0.32 × 0.13 × 0.13	0.18 × 0.11 × 0.10	0.49 × 0.32 × 0.18	0.26 × 0.19 × 0.11	
CCDC no.	774784	765333	774785	765323	765324	
space group	P $\bar{1}$	P $\bar{1}$	P $2_1/c$	P $2_1/c$	P $2_1/c$	
<i>a</i> (Å)	5.088(1)	5.091(1)	25.567(1)	25.595(6)	26.974(9)	
<i>b</i> (Å)	9.123(1)	9.264(1)	5.436(1)	5.388(1)	5.297(2)	
<i>c</i> (Å)	13.367(1)	13.411(2)	7.986(2)	8.183(2)	8.069(3)	
α (°)	105.304(5)	105.212(2)	90	90	90	
β (°)	98.725(5)	98.890(3)	98.554(3)	98.914(4)	93.089(6)	
γ (°)	99.351(5)	98.968(3)	90	90	90	
volume (Å ³)	578.0(1)	590.1(1)	1097.7(3)	1130.8(1)	1151.3(3)	
<i>Z</i>	2	2	4	4	4	
density (g cm ⁻³)	1.43	1.66	1.51	1.73	1.70	
μ (mm ⁻¹)	0.324	3.477	0.341	3.629	3.564	
<i>F</i> (000)	256.0	292.0	511.9	583.9	583.9	
$\theta_{\min, \max}$ (°)	2.4, 25.0	1.6, 26.0	1.6, 25.7	2.4, 25.5	2.3, 26.0	
<i>h</i> _{min, max}	-6, 5	-6, 6	-31, 30	-29, 31	-33, 32	
<i>k</i> _{min, max}	-10, 10	-11, 11	-6, 6	-6, 6	-6, 6	
<i>l</i> _{min, max}	-15, 15	-16, 16	-9, 9	-9, 9	-9, 9	
no. of reflections measured	8956	6172	14409	7932	11062	
no. unique reflections	2021	2309	2086	2092	2250	
no. of parameter	154	154	154	154	154	
<i>R</i> _{all} , <i>R</i> _{obs}	0.131, 0.090	0.042, 0.032	0.066, 0.040	0.044, 0.033	0.090, 0.050	
<i>wR</i> _{2_all} , <i>wR</i> _{2_obs}	0.249, 0.226	0.078, 0.075	0.105, 0.097	0.090, 0.087	0.124, 0.112	
$\Delta\rho_{\max, \min}$ (eÅ ⁻³)	0.987, -0.294	0.478, -0.203	0.228, -0.206	0.597, -0.406	0.742, -0.242	
GOF	0.967	1.070	1.039	1.070	1.041	

The next group of compounds considers the presence of a fluorine atom at the benzoyl ring with varying halogens on the amino side of the aromatic ring.

Group D (Set I). All compounds in this set are disordered and are discussed in a private communication.²⁰

Group D (Set II). 2FB-3ClA and 2FB-3BrA are isostructural and crystallize in noncentrosymmetric monoclinic *Pn* (*Pc*) space group with *Z* = 2 (Table 11). Along with usual intramolecular C—H···O (involving H13), the molecular conformation is stabilized by additional N—H···F (involving H1) intramolecular interaction. Indeed, the N—H···F interaction forms a six-membered intramolecular motif (Figure 10). The routine N—H···O hydrogen bond forms a chain along the *b*-axis. In 2FB-3ClA, C—H···F and C—H···Cl interactions provide further stability to the packing generating a wavelike assembly of molecules (Figure 11). It is of interest to note that in 2FB-3BrA, there is a C—Br···π interaction replacing the possible C—H···Br interactions (Figure 12; Table 12). However, the packing feature remains invariant.

Group D (Set III). The chloro and iodo compounds [2FB-4ClA and 2FB-4IA] in this set also do not form good quality crystals for diffraction studies. 2FB-4BrA crystallizes in noncentrosymmetric orthorhombic space group *Pca*₁ with *Z* = 4 (Table 11). Again, six-membered N—H···F intramolecular interaction stabilizes the molecular conformation. Once again N—H···O hydrogen bonds form molecular chains along the *b*-axis. Additional weak C—H···π (involving H6) and C—Br···π interactions hold the molecule together (Figure 13, Table 12).

Group E (Set I). 3FB-2ClA crystallizes in centrosymmetric monoclinic space group *P2*₁/*n* with *Z* = 4 (Table 13). Intramolecular C—H···O interaction confines the conformation of the molecule. N—H···O hydrogen bonds form molecular chain along the *a*-axis. The packing in the crystal lattice is mainly through C—Cl···π in 3FB-2ClA and C—Br···π in 3FB-2BrA (Figure 14). It is to be noted that both the packing features are almost similar except that the chlorine compound has short F···F interactions, whereas the bromine compound has C—H···F

interactions which further stabilize the packing of the molecule in the crystal lattice (Figure 14, Tables 14 and 15).

Group E (Set II). 3FB-3ClA and 3FB-3BrA crystallize in centrosymmetric monoclinic space group $P2_1/n$ with $Z = 4$ and are isostructural (Table 13). In addition to the intramolecular C–H \cdots O (involving H13) interaction, the N–H \cdots O (involving H1) hydrogen bond form a molecular chain along the

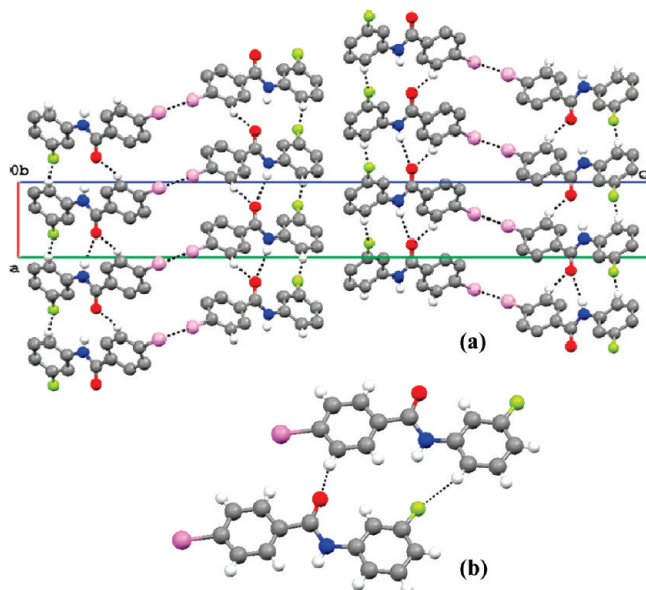


Figure 7. 3FA-4ClB and 3FA-4BrB show (a) homo-halogen X \cdots X (Cl, and Br) interaction acting as a link between the parallel chains formed by N–H \cdots O, C–H \cdots O and C–H \cdots F hydrogen bonds (b) C–H \cdots O and C–H \cdots F hydrogen bond depicting hetero-dimer formation.

Table 9. Intra- and Intermolecular Interactions^a

	D–H \cdots A	D \cdots H/Å	D \cdots A/Å	H \cdots A/Å	\angle D–H \cdots A/°	symmetry
4FA-2ClB	C13–H13 \cdots O1	0.93	2.881(6)	2.44	109	x, y, z
	N1–H1 \cdots O1	0.86	2.889(5)	2.09	154	$1+x, y, z$
	C5–H5 \cdots F1	0.93	3.225(7)	2.62	126	$x, y, z+1$
4FA-2BrB	C13–H13 \cdots O1	0.93	2.878(3)	2.43	109	x, y, z
	N1–H1 \cdots O1	0.86	2.892(3)	2.10	153	$-1+x, y, z$
	C5–H5 \cdots F1	0.93	3.298(7)	2.66	126	$x, y, z+1$
4FA-3ClB	C13–H13 \cdots O1	0.93	2.940(3)	2.47	112	x, y, z
	N1–H1 \cdots O1	0.86	3.300(2)	2.46	165	$x, -1+y, z$
	C3–H3 \cdots Cg1	0.93	3.623(3)	2.92	134	$x, -1/2-y, -1/2+z$
	C6–H6 \cdots Cg1	0.93	3.660(3)	2.96	133	$x, 1/2-y, 1/2+z$
	C10–H10 \cdots Cg2	0.93	3.649(3)	2.98	131	$x, -1/2-y, 1/2+z$
	C13–H13 \cdots Cg2	0.93	3.665(2)	2.98	132	$x, 1/2-y, -1/2+z$
4FA-3BrB	C13–H13 \cdots O1	0.93	2.940(4)	2.48	111	x, y, z
	N1–H1 \cdots O1	0.86	3.255(3)	2.41	166	$x, 1+y, z$
	C3–H3 \cdots Cg1	0.83	3.648(3)	2.94	134	$x, 3/2-y, 1/2+z$
4FA-4BrB	C13–H13 \cdots O1	0.93	2.942(5)	2.50	109	x, y, z
	N1–H1 \cdots O1	0.86	3.164(4)	2.33	164	$x, 1+y, z$
	C3–H3 \cdots Cg1	0.93	3.641(5)	2.90	137	$x, 3/2-y, 1/2+z$
	C6–H6 \cdots Cg1	0.93	3.610(5)	2.91	133	$x, 1/2-y, -1/2+z$
	C10–H10 \cdots Cg2	0.93	3.622(5)	2.93	132	$x, 3/2-y, -1/2+z$
	C13–H13 \cdots Cg2	0.93	3.656(4)	2.95	133	$x, 1/2-y, 1/2+z$

^a Cg1 = centroid of C1–C6 atom, Cg2 = centroid of C8–C13 atom.

b-axis. Further hetero-halogen F \cdots Cl/Br contact of Type II [$\theta_1 \approx 165^\circ, \theta_2 \approx 92^\circ$] strengthens the molecular assembly generating a staircase-like arrangement (Figure 15, Tables 14 and 15).

Group E (Set III). Compounds belonging to these sets are either disordered²⁰ or do not yield X-ray diffraction quality crystals.

Group F (Set I). 4FB-2ClA, 4FB-2BrA, and 4FB-2IA crystallize in centrosymmetric monoclinic space group $P2_1/c$, $P2_1/n$, and $P2_1/c$ respectively with $Z = 4$ (Table 16). Intramolecular C–H \cdots O interaction stabilizes the solid-state conformation for 4FB-2ClA and 4FB-2BrA. The N–H \cdots O hydrogen bonds form chains along the b-axis for 4FB-2ClA and 4FB-2BrA, whereas it is along the c-axis for 4FB-2IA. In case of 4FB-2ClA, additional C–H \cdots O (involving H6) and C–H \cdots Cl (involving H3) interactions form a dimer layer arrangement (Figure 16). A similar C–H \cdots O dimer also is observed in 4FB-2BrA; however, an additional hetero-halogen Br \cdots F Type II [$\theta_1 \approx 161^\circ, \theta_2 \approx 88^\circ$] interaction which links the N–H \cdots O parallel chains results in a different packing feature (Figure 17). 4FB-2IA is again different with C–I \cdots π chains

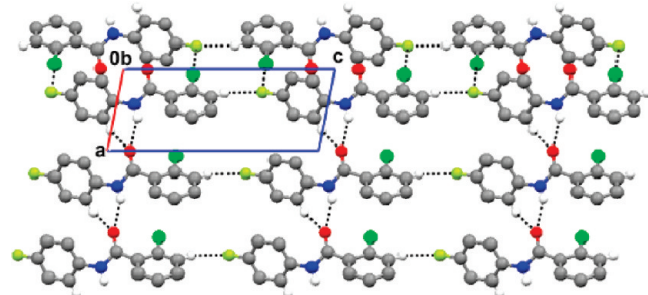


Figure 8. N–H \cdots O, C–H \cdots F hydrogen bond chains, and F \cdots Cl/Br interactions form layered packing for 4FA-2ClB and 4FA-2BrB.

Table 10. Halogen···Halogen Short Contact

	C—X···Y—C	X···Y/Å	∠C—X···Y/°	∠C—Y···X/°	symmetry	type
4FA-2ClB	C11—F1···Cl1—C6	3.189(4)	109	177	$-x, -y + 1, -z$	II
4FA-2BrB	C6—Br1···F1—C11	3.160(2)	178	108	$-x, -y + 1, -z + 1$	II
4FA-3ClB	C11—F1···F1A—C11A	2.963(2)	107	112	$-x + 1, y - 1/2, -z + 3/2$	I
	C5—Cl1···Cl1—C5	3.609(1)	165	95	$-x, +y - 1/2, -z + 1/2$	II
4FA-3BrB	C11—F1···F1—C11	2.977(2)	107	113	$-x, +y + 1/2, -z + 1/2$	I
	C5—Br1···Br1—C5	3.706(2)	162	99	$-x + 1, y - 1/2, -z + 3/2$	II
4FA-4BrB	C4—Br1···Br1—C4	3.791(3)	121	149	$-x, +y - 1/2, -z + 3/2$	II
	C11—F1···F1—C11	2.962(3)	109	114	$-x + 1, y - 1/2, -z + 1/2$	I

Table 11. Crystallographic Information

	Set (II)		Set (III)
	2FB-3ClA	2FB-3BrA	2FB-4BrA
formula	C ₁₃ H ₉ NOFCl	C ₁₃ H ₉ NOFBr	C ₁₃ H ₉ NOFBr
formula weight	249.7	294.1	294.1
temperature K	292(2)	292(2)	292(2)
size of crystal (mm)	0.28 × 0.22 × 0.19	0.37 × 0.28 × 0.16	0.26 × 0.25 × 0.04
CCDC no.	774790	765325	765326
space group	Pn	Pc	Pca ₂ ₁
a (Å)	5.265(2)	4.779(3)	8.159(3)
b (Å)	4.503(1)	5.078(3)	5.302(2)
c (Å)	23.769(4)	23.792(1)	26.843(1)
α (°)	90	90	90
β (°)	94.293(8)	92.498(1)	90
γ (°)	90	90	90
volume (Å ³)	561.9(2)	576.9(2)	1161.3(2)
Z	2	2	4
density (g cm ⁻³)	1.48	1.69	1.68
μ (mm ⁻¹)	0.333	3.556	3.534
F(000)	256.0	292.0	583.9
θ _{min, max} (°)	1.7, 26.0	3.4, 25.3	3.0, 28.1
h _{min, max}	−6, 6	−5, 5	−9, 10
k _{min, max}	−4, 5	−6, 6	−6, 6
l _{min, max}	−29, 28	−28, 28	−34, 35
no. of reflections measured	8502	5077	9110
no. unique reflections	2157	2053	2723
no. of parameter	154	155	158
R _{all} , R _{obs}	0.039, 0.035	0.104, 0.077	0.104, 0.047
wR _{2_all} , wR _{2_obs}	0.084, 0.083	0.185, 0.171	0.108, 0.089
Δρ _{max, min} (e Å ⁻³)	0.204, −0.128	1.704, −0.405	0.389, −0.221
GOF	1.849	1.043	1.006

interconnected through C—H···F (involving H5) hydrogen bonds to form a “ladder like” arrangement (Figure 17). Additional C—H···O (involving H10) and C—H···π (involving H9) interactions enhance the stability of assembly in this structure (Table 17).

Group F (Set II). 4FB-3ClA and 4FB-3BrA crystallize in centrosymmetric monoclinic space group P₂₁/c with Z = 4 and are isostructural, whereas 4F-3IA crystallizes in centrosymmetric orthorhombic space group Pbc_a with Z = 8 (Table 16). In the case of 4FB-3ClA and 4FB-3BrA, the N—H···O hydrogen bonds form a molecular chain along the c-axis and the O1 forms bifurcated hydrogen bonds (involving H2 and H1). Additional

C—H···O, C—H···π along with π···π interactions stabilize and force the molecules to arrange in a manner such that there are no halogen interactions (Figure 18). 4FB-3IA is different and prefers halogen involved interactions. N—H···O hydrogen bonds form infinite molecular chain along the b-axis. C—I···π and C—H···F interactions form parallel chains individually. It is to be noted that additionally, the C—H···π and π···π stacks also stabilize the molecular packing. Two consecutive C—I···π and C—H···F interactions form a helical structure along the b-axis (Table 17, Figure 19).

Group F (Set III). 4FB-4ClA crystallizes in centrosymmetric monoclinic space group P₂₁/c with Z = 4 (Table 16).

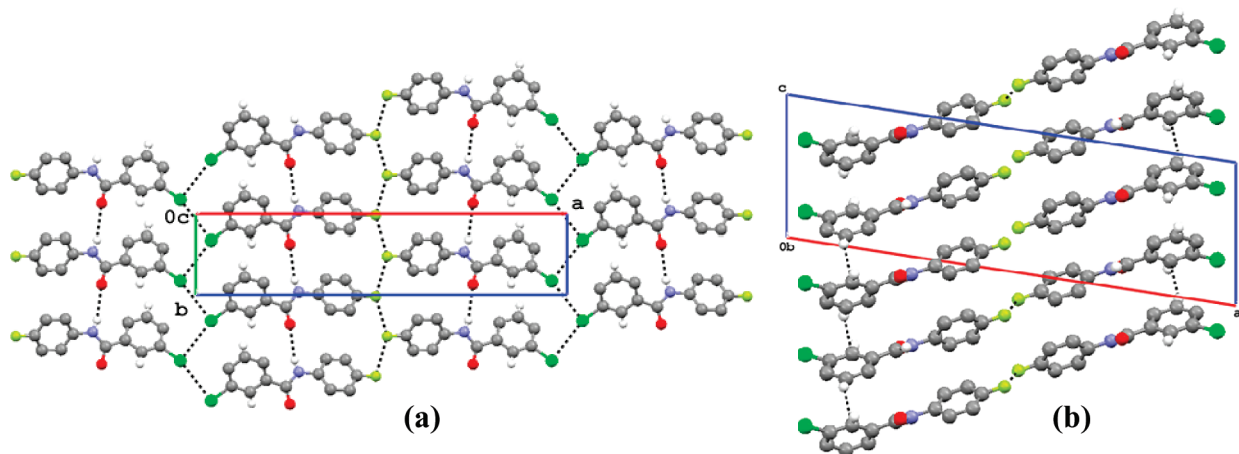


Figure 9. 4FA-3ClB and 4FA-3BrB show (a) $\text{N}-\text{H}\cdots\text{O}$, $\text{F}\cdots\text{F}$, and $\text{Cl}/\text{Br}\cdots\text{Br}/\text{Cl}$ form parallel hydrogen bond chains, and (b) the $\text{C}-\text{H}\cdots\pi$ chain forms a separate layered structure.

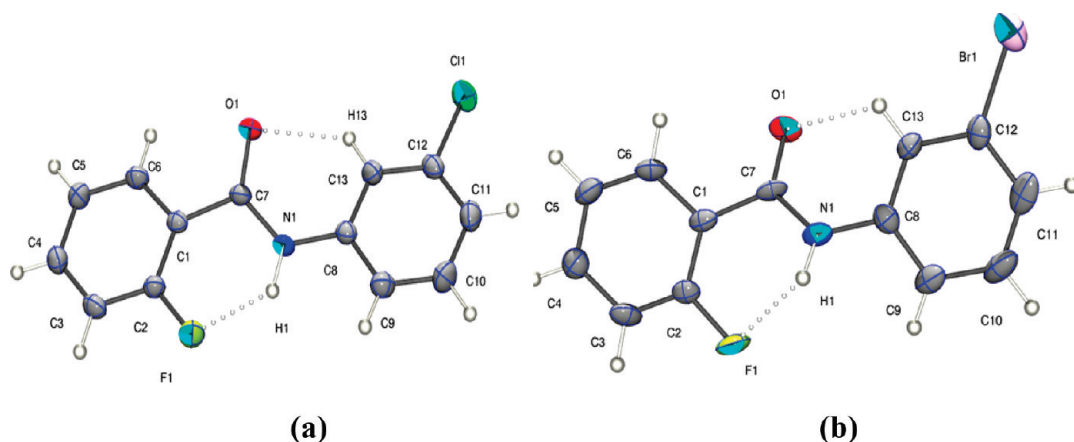


Figure 10. ORTEP drawn with 30% ellipsoid probability depicting six-membered $\text{N}-\text{H}\cdots\text{F}$ and $\text{C}-\text{H}\cdots\text{O}$ intramolecular interactions as dotted lines (a) 2FB-3ClA (b) 2FB-2BrA.

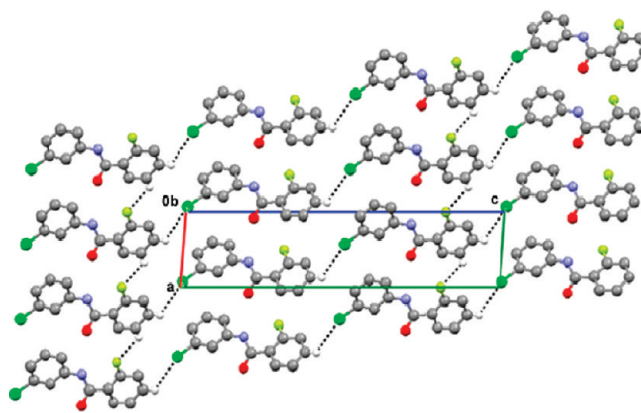


Figure 11. 2FB-3ClA shows a wavelike assembly of $\text{C}-\text{H}\cdots\text{Cl}$ and $\text{C}-\text{H}\cdots\text{F}$ interactions.

Intramolecular $\text{C}-\text{H}\cdots\text{O}$ (involving H13) is present forming a six-membered ring and $\text{N}-\text{H}\cdots\text{O}$ hydrogen bonds form molecular chain which is further assisted by $\text{C}-\text{H}\cdots\text{O}$ (involving H2), $\text{C}-\text{H}\cdots\text{F}$ (involving H6), and $\pi\cdots\pi$ stacking. In addition, homo-halogen $\text{Cl}\cdots\text{Cl}$ directional contacts of Type I [3.35 Å,

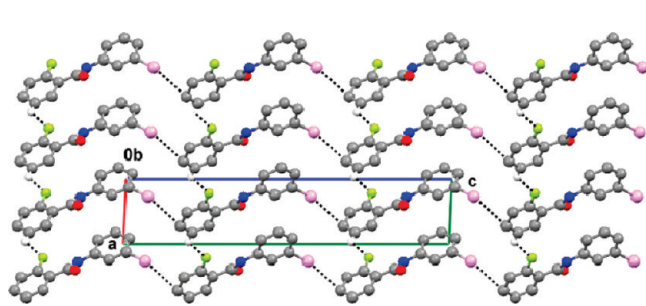


Figure 12. 2FB-3BrA shows a wavelike assembled pattern through edge $\text{C}-\text{Br}\cdots\pi$ and $\text{C}-\text{H}\cdots\text{F}$ interactions.

$\theta_1 = \theta_2 \approx 153^\circ$] enhance the stability of packing. The participation of all interactions forms an unusual “cone type” arrangement along the c -axis (Figure 20; Tables 17 and 18). 4FB-4BrA crystallizes in non-centrosymmetric orthorhombic space group $P2_12_12$ ($Z = 8$) with $Z' = 2$. $\text{C}-\text{H}\cdots\text{O}$ (involving H13 and H13') interactions stabilize the molecular conformation and $\text{N}-\text{H}\cdots\text{O}$ (involving H1 and H1') hydrogen bonds form molecular chain along the c -axis. The $\text{C}-\text{H}\cdots\text{F}$ (involving H5) and $\text{C}-\text{H}\cdots\pi$ (involving

Table 12. Intra- and Intermolecular Interactions^a

crystal	D—H···A	D···H/Å	D···A/Å	H···A/Å	∠D—H···A/°	symmetry
2FB-3CIA	N1—H1···F1	0.86	2.752(2)	2.15	127	<i>x, y, z</i>
	C13—H13···O1	0.93	2.878(3)	2.35	115	<i>x, y, z</i>
	N1—H1···O1	0.86	3.128(2)	2.41	142	$-1 + x, y, z$
	C4—H4···Cl1	0.93	3.611(3)	2.97	127	$x - 1/2, -y + 1, z + 1/2$
	C5—H5···F1	0.93	3.295(3)	2.66	125	$x - 1, y, z$
2FB-3BrA	N1—H1···F1	0.86	2.748(1)	2.17	124	<i>x, y, z</i>
	C13—H13···O1	0.93	2.904(1)	2.40	114	<i>x, y, z</i>
	N1—H1···O1	0.86	2.973(2)	2.23	144	$x, -1 + y, z$
	C5—H5···F1	0.93	3.313(3)	2.63	130	$x + 1, y, z$
	C12—Br1···C4		5.323(3)	3.510(2)	161	
2FB-4BrA	N1—H1···F1	0.86	2.750(5)	2.15	126	<i>x, y, z</i>
	N1—H1···O1	0.86	3.198(5)	2.41	151	$x, 1 + y, z$
	C6—H6···Cg1		3.589(6)	2.93	129	$1/2 + x, 1 - y, z$
	C11—Br1···C5		5.527(4)	3.70	159	$-x + 2, -y + 1, z - 1/2$

^a Cg1 = centroid of C1—C6 ring.

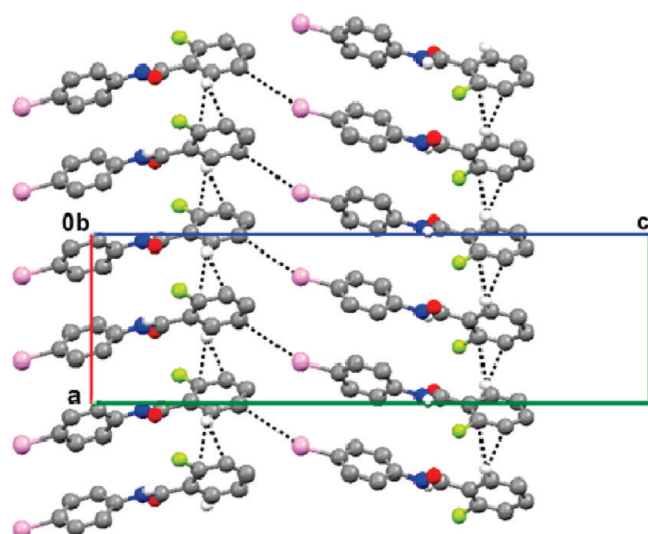


Figure 13. 2F-4BrA form C—H···π chains interconnected through edge C—Br···π directional contact.

H13', H12, H10', H6, H6' and H3') interactions enhance the stability of packing. The presence of C—H···π appears to weaken the homo-halogen···halogen interactions though the directionality is maintained (Figure 21, Tables 17 and 18).

DISCUSSION

The analysis of all the structures studied in Tables 2, 5, 8, 11, 13 and 16 brings out a few generalizations in halogen-substituted benzanilides. It is also of interest to compare the present series of crystal and molecular structure determinations on mixed-halogenated benzanilides with the parent compound, that is, the unsubstituted benzanilide³⁰ along with fluoro-³¹ and chloro-substituted benzanilides.¹⁷ It is already well established that the prediction of crystal structure of a compound, given its molecular connectivity diagram, is still in its fancy. There are two important questions which need to be addressed when one is dealing with a large number of isomeric molecules which are obtained by simply varying the position of the functional group

over different positions of the molecule, that is, changes in molecular conformation and also the modifications associated with crystal packing. Furthermore, isostructural³² plays a very important role because it so happens that in certain cases changing the position of an atom in the molecule does not lead to any changes in the crystal packing, whereas in certain cases there is a pronounced change in crystal packing. These issues are further complicated by the appearance of polymorphs in such molecules which again contributes to the complexity associated with small molecules whose crystal structures are being determined. The weak, soft, and flexible weak interactions play a pivotal role in crystal nucleation and growth processes resulting in different physical forms and structures having multiple molecules in the asymmetric unit (high Z').³³ The area of crystal engineering has this limitation wherein we can make a conceptual prediction from the available structural data for a series of molecules (containing a given molecular framework), but there is no answer to what will be the observed when a given functional group is changed in a given position or moved over different portions of the molecule, this inability being due to the lack of a robust crystal structure prediction model which will relate the molecular structure with the crystal structure. Keeping in mind the above-mentioned limitations, it is indeed noteworthy to explore the supramolecular attributes which accompany such crystallographic determinations in terms of changes in molecular conformation, crystal packing, isostructurality, and elucidating the diversity associated with weak interactions.

The changes in molecular conformation associated with different halogen atoms follow certain trends. The dihedral angles between plane1—plane2 lies between 2 and 6° for all the compounds in Group A (Table S1, Supporting Information: Set I, II, III [fluoro in ortho position]; except 2FA-2BrB) indicating planarity assisted by electron delocalization between the benzoyl moiety and the amido functional group. A similar feature is observed for Set III (Group B). However, the presence of a fluorine atom at the para position of the aniline ring results in loss of parallelism and the corresponding dihedrals between plane1—plane2 lie in the range of 60–80° [Table S1, Supporting Information: Group C, Set I, II, III]. Thus, the electronic features play an important role in deciding the equilibrium geometry.

Table 13. Crystallographic Information

	Set (I)		Set (II)	
	3FB-2ClA	3FB-2BrA	3FB-3ClA	3FB-3BrA
formula	C ₁₃ H ₉ NOFCl	C ₁₃ H ₉ NOFBr	C ₁₃ H ₉ NOFCl	C ₁₃ H ₉ NOFBr
formula weight	249.7	294.1	249.7	294.1
temperature K	292(2)	292(2)	292(2)	292(2)
size of crystal (mm)	0.21 × 0.07 × 0.06	0.24 × 0.16 × 0.10	0.22 × 0.12 × 0.11	0.15 × 0.12 × 0.1
CCDC no.	774788	640040	774791	765327
space group	P ₂ ₁ /n			
a (Å)	4.881(2)	11.178(1)	14.983(2)	15.198(6)
b (Å)	11.574(1)	4.768(5)	4.910(2)	4.903(2)
c (Å)	19.951(2)	21.824(2)	15.414(2)	15.498(2)
α (°)	90	90	90	90
β (°)	92.255(1)	94.714(2)	93.383(2)	93.949(7)
γ (°)	90	90	90	90
volume (Å ³)	1126.3(1)	1159.4(3)	1131.9(1)	1152.2(3)
Z	4	4	4	4
density (g cm ⁻³)	1.47	1.68	1.46	1.70
μ (mm ⁻¹)	0.333	3.539	0.331	3.562
F (000)	511.9	583.9	511.9	583.9
θ _{min, max} (°)	2.0, 26.0	1.9, 25.7	1.8, 26.0	1.8, 26.0
h _{min, max}	-6, 6	-13, 13	-18, 18	-18, 18
k _{min, max}	-14, 14	-5, 5	-6, 6	-6, 6
l _{min, max}	-24, 24	-26, 26	-19, 19	-19, 18
no. of reflections measured	11458	8253	10757	11288
no. unique reflections	2202	2192	2213	2254
no. of parameter	154	154	154	154
R _{all} , R _{obs}	0.064, 0.046	0.041, 0.031	0.067, 0.055	0.082, 0.054
wR ₂ _{all} , wR ₂ _{obs}	0.115, 0.108	0.073, 0.069	0.143, 0.135	0.117, 0.109
Δρ _{max, min} (e Å ⁻³)	0.387, -0.231	0.357, -0.284	0.433, -0.266	0.575, -0.314
GOF	1.095	1.036	1.070	1.097

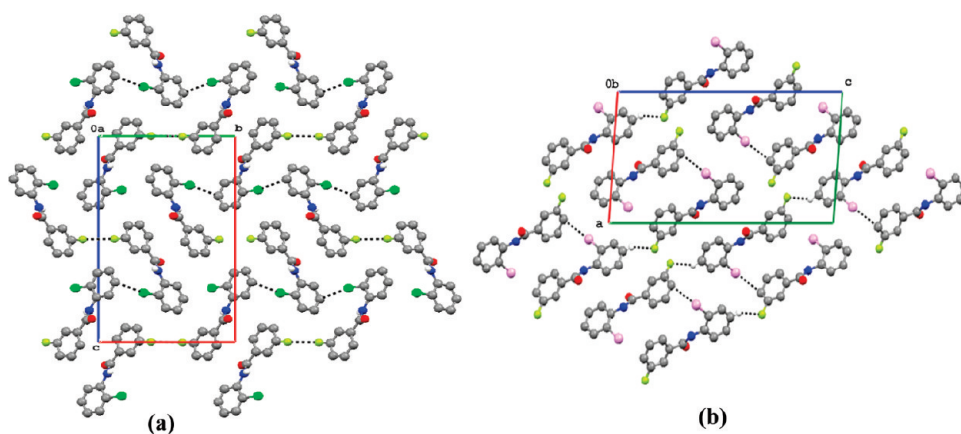


Figure 14. 3FB-2ClA prefers edge C—Cl···π and F···F, whereas 3FB-2BrA prefers C—Br···π and C—H···F interactions.

The appearance of a six-membered C—H···O intramolecular interaction in almost all crystal structures discussed above indicates that this particular interaction stabilizes the molecular conformation. The reason appears to be essentially geometrical as the N—H group prefers to be trans to the C=O group. In those cases where intramolecular C—H···O interactions are not present (as decided based on distance between H···O and angle

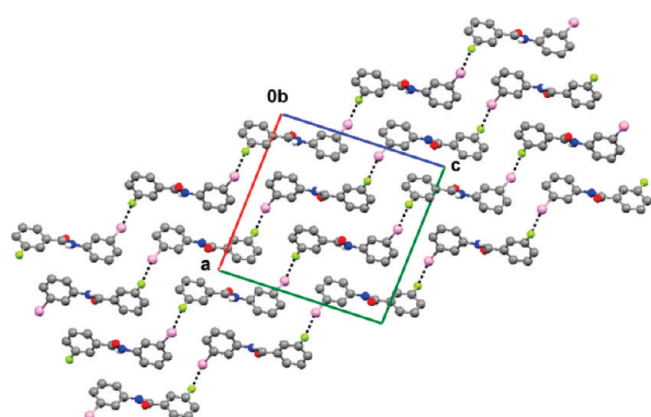
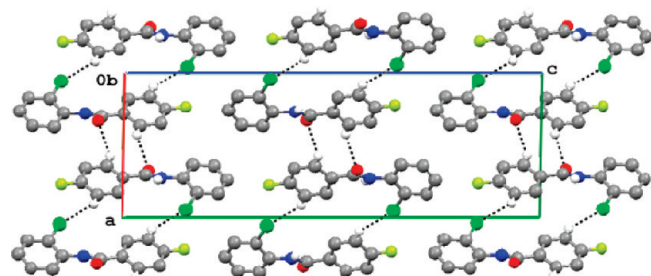
C—H···O), additional halogen involved contacts appear to keep the molecular conformation intact, for example, in 2FA-2ClB, 2FB-4BrA, and 4FB-3IA. N—H···F intramolecular interactions have been extensively studied in recent times as possible interactions rigidifying molecular conformation.^{12,13} The presence of six-membered N—H···F intramolecular interaction is observed in structures 2FB-3ClA, 2FB-3BrA, and 2FB-4BrA. Such

Table 14. Intra- and Intermolecular Interactions

crystal	D—H···A	D···H/Å	D···A/Å	H···A/Å	$\angle D\text{—H}\cdots A/^\circ$	symmetry
3FB-2CIA	C13—H13···O1	0.93	2.909(3)	2.46	110	x, y, z
	N1—H1···O1	0.86	2.900(2)	2.11	153	$-1 + x, y, z$
	C9—Cl1···C12		5.414(3)	3.415(1)	168	$1/2 - x, 1/2 + y, 1/2 - z$
3FB-2BrA	C13—H13···O1	0.93	2.921(3)	2.48	110	x, y, z
	N1—H1···O1	0.86	2.915(3)	2.16	147	$x, -1 + y, z$
	C9—Br1···C4		4.054(3)	3.36	170	$x, -1 + y, z$
	C11—H11···F1	0.93	3.406(1)	2.57	148	$-x, -y + 1, -z$
3FB-3CIA	C13—H13···O1	0.93	2.880(3)	2.44	109	x, y, z
	N1—H1···O1	0.86	2.879(2)	2.08	154	$x, -1 + y, z$
3FB-3BrA	C13—H13···O1	0.93	2.882(6)	2.44	109	x, y, z
	N1—H1···O1	0.86	2.868(4)	2.07	153	$x, -1 + y, z$

Table 15. Halogen···Halogen Short Contact

crystal	C—X···Y—C	X···Y/Å	$\angle C\text{—X}\cdots Y/^\circ$	$\angle C\text{—Y}\cdots X/^\circ$	symmetry	type
3FB-2CIA	C3—F1···F1—C3	2.918(2)	159	159	$-x + 1, -y, -z + 1$	I
3FB-3CIA	C12—Br1···F1—C3	3.251(2)	165	92	$x - 1/2, -y + 1/2, z + 1/2$	II
3FB-3BrA	C12—Br1···F1—C3	3.263(3)	165	92	$x - 1/2, -y + 1/2, z + 1/2$	II

**Figure 15.** 3F-3CIA and 3F-3BrA prefer hetero-halogen Cl/Br···F interaction to form a staircase arrangement.**Figure 16.** 4FB-2CIA prefers the alternate dimer arrangement through C—H···Cl and C—H···O interactions.

interactions have been characterized in detail using NMR and DFT studies performed on fluorinated benzanilides.³⁴

The mixed halogenated compounds exhibit isostructurality in the solid state and depending on the nature of intermolecular

interactions crystallize in a variety of space groups (both centrosymmetric and noncentrosymmetric) belonging either to the triclinic, monoclinic, and orthorhombic crystal system, respectively. The following series of compounds are isostructural to each other having similarity in molecular conformation and crystal packing: Group A: Set II (2FA-3ClB, 2FA-3BrB); Set III: (2FA-4ClB, 2FA-4BrB, 2FA-4IB). Group B: Set III (3FA-4ClB, 3FA-4BrB, 3FA-4IB). Group C: Set I (4FA-2ClB, 4FA-2BrB); Set II (4FA-3ClB, 4FA-3BrB, 4FA-4BrB). Group D: Set II (2FB-3CIA, 2FB-3BrA); Group E: Set II (3FB-3CIA, 3FB-3BrA).

The interaction of utmost importance in the formation of supramolecular assemblies in these benzanilides is the N—H···O hydrogen bond. Indeed, this interaction forms chains in the crystal lattice essentially along a particular crystallographic axis. The supporting interactions, involving halogens, like for example C—H···X, C—X···π, and X···X, develop depending on the size of the halogen atom. It is also to be noted that in the case of compounds which display C—H···O, C—H···π, and π···π interactions, the propensity of formation of halogen interactions get reduced; more often than not in these cases halogens appear at distances more than the sum of van der Waals radii.³⁵ However, the geometry still appears to be favorable. F and Cl prefer to have C—H···F and C—H···Cl contact, whereas Br and I prefer to have C—Br···π and C—I···π interactions.

There is a higher propensity for the formation of homo-halogen···halogen interactions in comparison to hetero-halogen···halogen interactions. 4FA-2ClB and 4FA-2BrB form Cl···F and Br···F short hetero-halogen contacts in the crystal lattice. The heavy halogens are polarized in the polar region (along the C—X vector) having a positive electrostatic potential and a negative electrostatic potential in the equatorial region (perpendicular to the C—X vector). The atomic size, polarization, and radial anisotropy increase in the order Cl < Br < I, whereas electronegativity changes are in the reverse order.³⁶ Thus, in the case of unsymmetrical interhalogen interactions, for

Table 16. Crystallographic Information

	Set (I)			Set (II)			Set (III)	
	4FB-2ClA	4FB-2BrA	4FB-2IA	4FB-3ClA	4FB-3BrA	4F-3IA	4FB-4ClA	4FB-4BrA
formula	C ₁₃ H ₉ NOFCl	C ₁₃ H ₉ NOFBr	C ₁₃ H ₉ NOFI	C ₁₃ H ₉ NOFCl	C ₁₃ H ₉ NOFBr	C ₁₃ H ₉ NOFI	C ₁₃ H ₉ NOFCl	C ₁₃ H ₉ NOFBr
formula weight	249.7	294.1	341.1	249.7	294.1	341.1	249.7	294.1
temperature K	292(2)	292(2)	292(2)	292(2)	292(2)	292(2)	292(2)	292(2)
size of crystal (mm)	0.28 × 0.23 × 0.19	0.56 × 0.10 × 0.07	0.27 × 0.24 × 0.21	0.29 × 0.22 × 0.21	0.37 × 0.27 × 0.1	0.28 × 0.23 × 0.18	0.28 × 0.21 × 0.18	0.27 × 0.15 × 0.44
CCDC no.	774789	640038	774781	774778	765328	774782	774779	640041
space group	P ₂ 1/c	P ₂ 1/n	P ₂ 1/c	P ₂ 1/c	P ₂ 1/c	Pbc _a	P ₂ 1/c	P ₂ 1 ₂ 1 ₂
<i>a</i> (Å)	9.104(3)	15.691(2)	18.774(4)	12.650(1)	12.809(2)	9.201(1)	12.095(2)	15.276(2)
<i>b</i> (Å)	4.826(1)	4.764(2)	7.107(2)	9.531(1)	9.619(1)	9.941(1)	9.7867(1)	28.568(4)
<i>c</i> (Å)	26.011(2)	16.528(2)	9.282(2)	9.989(3)	10.009(1)	27.444(2)	9.912(2)	5.346(2)
α (°)	90	90	90	90	90	90	90	90
β (°)	90.940(3)	107.697(2)	93.284(5)	102.072(2)	103.343(2)	90	93.510(6)	90
γ (°)	90	90	90	90	90	90	90	90
volume (Å ³)	1142.8(1)	1177.1(2)	1236.4(2)	1177.8(1)	1199.9(3)	2510.3(2)	1171.1(2)	2333.09(6)
<i>Z</i>	4	4	4	4	4	8	4	8
density (g cm ⁻³)	1.45	1.66	1.83	1.41	1.63	1.80	1.42	1.67
μ (mm ⁻¹)	0.328	3.486	2.584	0.318	3.420	2.546	0.320	3.518
<i>F</i> (000)	511.9	583.9	655.9	511.9	583.9	1311.9	511.9	1167.8
$\theta_{\min, \max}$ (°)	3.1, 26.0	1.6, 26.0	1.1, 25.7	2.7, 26.0	2.7, 25.5	1.5, 25.0	3.3, 26.0	1.4, 25.0
<i>h</i> _{min, max}	-11, 11	-17, 19	-22, 22	-15, 14	-15, 15	-10, 9	-14, 14	-18, 18
<i>k</i> _{min, max}	-5, 5	-5, 5	-8, 6	-11, 11	-11, 11	-11, 10	-12, 12	-33, 33
<i>l</i> _{min, max}	-32, 32	-20, 20	-7, 11	-7, 12	-12, 12	-32, 32	-12, 12	-6, 6
no. of reflections measured	11776	8598	9312	8929	11587	10147	9368	22379
no. unique reflections	2240	2304	2359	2317	2222	2201	2299	4114
no. of parameter	154	154	155	155	158	154	154	307
<i>R</i> _{all} , <i>R</i> _{obs}	0.063, 0.047	0.066, 0.045	0.057, 0.040	0.066, 0.046	0.051, 0.035	0.068, 0.043	0.084, 0.044	0.088, 0.049
<i>wR</i> _{2_all} , <i>wR</i> _{2_obs}	0.133, 0.127	0.123, 0.115	0.116, 0.095	0.157, 0.135	0.087, 0.083	0.110, 0.096	0.115, 0.105	0.136, 0.107
$\Delta\rho_{\max, \min}$ (e Å ⁻³)	0.619, -0.265	0.874, -0.437	0.788, -0.437	0.254, -0.259	0.516, -0.489	1.726, -1.350	0.147, -0.233	0.707, -0.449
GOF	1.033	1.012	1.162	1.118	1.030	1.030	0.894	1.042

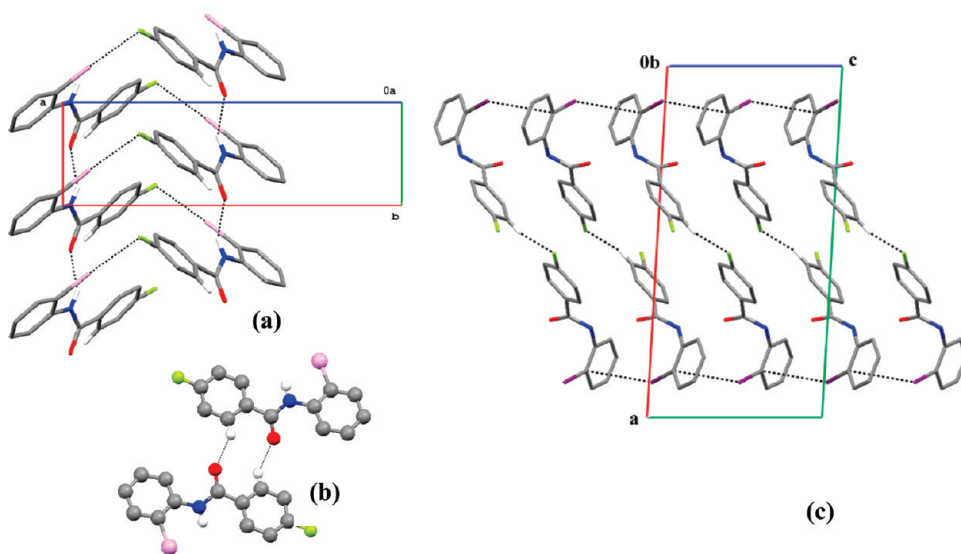


Figure 17. (a) 4FB-2BrA show hetero-halogen Br...F short contact which links the N—H...O parallel infinite chains and (b) weak C—H...O dimer arrangement, (c) 4FB-2IA forms C—I...π molecular chains which are interconnected through C—H...F interactions.

Table 17. Intra- and Intermolecular Interactions^a

crystal	D—H···A	D···H/Å	D···A/Å	H···A/Å	∠D—H···A/°	symmetry
4FB-2CIA	C13—H13···O1	0.93	2.902(3)	2.47	109	<i>x, y, z</i>
	N1—H1···O1	0.86	2.920(2)	2.13	153	<i>x, -1 + y, z</i>
	C6—H6···O1	0.93	3.461(3)	2.64	146	$-x + 1, -y + 1, -z + 1$
4FB-2BrA	C13—H13···O1	0.93	2.895(5)	2.43	111	<i>x, y, z</i>
	N1—H1···O1	0.86	2.880(4)	2.13	145	<i>x, -1 + y, z</i>
	C6—H6···O1	0.93	3.471(3)	2.67	146	$-x + 1, -y + 1, -z + 1$
4FB-2IA	N1—H1···O1	0.86	2.937(4)	2.10	166	<i>x, 3/2 — y, -1/2 + z</i>
	C5—H5···F1	0.93	3.335(8)	2.51	148	$1 - x, -1/2 + y, 3/2 - z$
	C10—H10···O1	0.93	3.418(7)	2.60	144	$-x, -y + 2, -z + 1$
	C13—H1···Cg2		5.442(5)	3.620(2)	143	<i>x, 3/2 — y, 1/2 + z</i>
	C9—H9···Cg1	0.93	3.702(6)	2.84	154	<i>x, 3/2 — y, -1/2 + z</i>
4FB-3CIA	N1—H1···O1	0.86	2.952(2)	2.13	159	<i>x, 3/2 — y, -1/2 + z</i>
	C2—H2···C13	0.93	3.525(1)	2.68	151	<i>x, -y + 1/2 + 1, z - 1/2</i>
	C2—H2···O1	0.93	3.370(3)	2.61	138	<i>x, -y + 1/2 + 1, z - 1/2</i>
	Cg1···Cg1		3.744(3)			$-x, 1 - y, -z$
	Cg2···Cg2		3.8771(1)			$-x, 2 - y, -z$
4FB-3BrA	N1—H1···O1	0.86	2.968(3)	2.18	164	<i>x, 1/2 — y, 1/2 + z</i>
	C2—H2···C13	0.93	3.520(2)	2.67	151	<i>x, -y + 1/2 + 1, z - 1/2</i>
	C2—H2···O1	0.93	3.398(3)	2.63	140	<i>x, -y + 1/2 + 1, z - 1/2</i>
	Cg1···Cg1		3.7558(1)			$-x, 1 - y, 1 - z$
	Cg2···Cg2		3.983(2)			$1 - x, -y, 1 - z$
4FB-3IA	N1—H1···O1	0.86	2.941(5)	2.12	160	$1/2 - x, 1/2 + y, z$
	C12—H1···Cg2		5.612(5)	3.54	168	$1 - x, -1/2 + y, 1/2 - z$
	C5—H5···F1	0.93	3.222(6)	2.63	122	$-x + 1/2, y - 1/2, z$
	C10—H10···Cg1	0.93	3.641(6)	2.93	134	$1 + x, y, z$
	Cg1···Cg1		3.744(3)			$-x, 1 - y, -z$
4FB-4CIA	C13—H13···O1	0.93	2.856(2)	2.37	113	<i>x, y, z</i>
	N1—H1···O1	0.86	2.881(2)	2.04	166	<i>x, 3/2 — y, 1/2 + z</i>
	C2—H2···O1	0.93	3.201(2)	2.49	133	<i>x, 3/2 — y, 1/2 + z</i>
	C6—H6···F1	0.93	3.494(3)	2.63	154	$-x, y - 1/2, -z + 1/2$
	Cg1···Cg1		3.685(1)			$-x, 2 - y, 1 - z$
4FB-4BrA	Cg2···Cg2		3.759(1)			$1 - x, 1 - y, 1 - z$
	N1—H1···O1	0.86	3.140(7)	2.34	154	<i>x, y, -1 + z</i>
	N1'—H1'···O1'	0.86	3.146(7)	2.34	155	<i>x, y, 1 + z</i>
	C13—H13···O1	0.93	2.899(7)	2.44	110	<i>x, y, z</i>
	C13'—H13'···O1'	0.93	2.921(7)	2.45	112	<i>x, y, z</i>
4FB-4CIA	C5H5···F1	0.93	3.310(7)	2.59	133	<i>x, y - 1, z - 1</i>
	C3'—H3'···Cg1	0.93	3.682(7)	2.98	134	$-1/2 + x, 1/2 - y, 2 - z$
	C6—H6···Cg4	0.93	3.650(7)	2.92	136	<i>x, y, 1 + z</i>
	C6'—H6'···Cg2	0.93	3.661(7)	2.93	137	<i>x, y, -1 + z</i>
	C10—H10···Cg3	0.93	3.659(7)	2.98	131	<i>x, y, z</i>
	C10'—H10'···Cg1	0.93	3.595(7)	2.92	130	<i>x, y, z</i>
	C12—H12···Cg4	0.93	3.578(7)	2.92	129	$1/2 + x, 1/2 - y, 2 - z$
	C13'—H13'···Cg2	0.93	3.571(7)	2.92	129	$-1/2 + x, 1/2 - y, 1 - z$

^a Cg1 = centroid of C1—C6 ring, Cg2 = centroid of C8—C13 ring, Cg3 = centroid of C1'—C6'. Cg4 = centroid of C5'—C13' ring.

Table 18. Halogen···Halogen Short Contact

	C—X···Y—C	X···Y/Å	∠C—X···Y/°	∠C—Y···X/°	symmetry	type
4FB-2BrA	C9—Br1···F1—C3	3.265(1)	161	88	$-x + 1/2, +y - 1/2, -z + 3/2$	II
4FB-4CIA	C11—Cl1···Cl1—C11	3.356(2)	153	153	$-x + 1, -y, -z + 1$	I
4FB-4BrA	C11—Br1···Br1'—C11'	3.741(2)	133	138	<i>x, y, z - 1</i>	I
	C4—F1···F1'—C4'	2.952(1)	104	120	<i>x, y + 1, z</i>	I

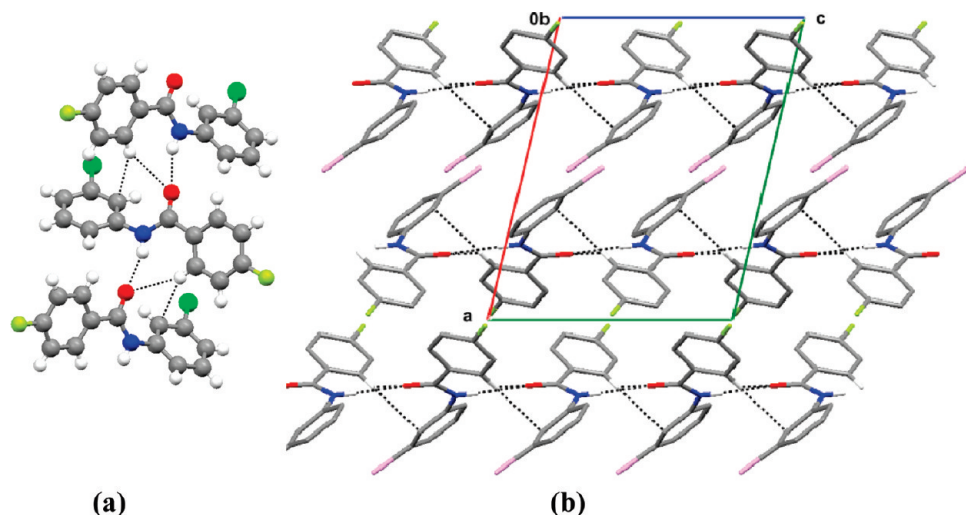


Figure 18. 4FB-3ClA and 4FB-3BrA prefer (a) bifurcated C–H \cdots O and C–H \cdots π interactions, (b) lead to cross folded geometry with N–H \cdots O and $\pi\cdots\pi$ stacking without the participation of halogen interactions.

example, C–Cl \cdots F–C, the negative equatorial part of the lighter halogen fluorine preferentially approaches the positive polar region of the heavier halogen bromine³⁷ and hence the observed Type II geometry. Furthermore, 3FB-3ClA and 3FB-3BrA also exhibit such intermolecular hetero-halogen contacts. It has been observed that halogen \cdots halogen contacts direct non-centrosymmetric packing of dipolar organic molecules in the solid state involving different geometrical arrangements,³⁸ and a similar packing feature is observed in the present halogen-substituted benzanilides wherein in addition to strong N–H \cdots O hydrogen bonds, intermolecular homo-halogen \cdots halogen contacts direct packing of molecules into noncentrosymmetric environments [2FA-4ClB, 2FA-4BrB, 2FA-4IB have Cl \cdots Cl, Br \cdots Br, I \cdots I short contact that orient molecules along the 2_1 screw axis which are orthogonal to the direction along which strong N–H \cdots O hydrogen bonds are formed, namely, the crystallographic *a* axis; 4FA-3ClB, 4FA-3BrB, 4FA-4BrB all have F \cdots F contacts (Type I) in addition to Cl \cdots Cl, Br \cdots Br, and I \cdots I intermolecular contact which direct packing of molecules along the 2_1 screw axis. However, the overall packing in these molecules is centrosymmetric; 3FB-3ClA and 3FB-3BrA form Type II interhalogen contact along the [101] crystallographic direction utilizing the *n*-glide plane as the symmetry element, the overall packing being centrosymmetric. A large number of benzanilides containing multiple chlorine atoms on different positions of the two aromatic phenyl rings have been synthesized, and their crystal and molecular structures were determined.¹⁷ In addition to the well-characterized N–H \cdots O hydrogen bond, short contacts involving different chlorine atoms have been observed in one such case, that is, in 4-chloro-*N*-(2,6-dichlorophenyl)-benzamide. This molecule crystallizes with four molecules in the asymmetric unit and contains the homo-halogen Cl \cdots Cl short contact of 3.408(1) \AA [17(x)]. These investigations performed on chlorine containing benzanilides again point to the complexity associated with prediction of crystal structures for closely related molecules and the nature of the interactions, symmetry, and molecular conformation which they adopt.

It is to be mentioned that F \cdots F contacts prefer Type I geometry, while the contacts involving heavier halogens, namely, Cl \cdots Cl, Br \cdots Br, and I \cdots I prefer to have Type II geometry.

Hetero-halogen \cdots halogen interactions on the other hand are predominately of Type II geometry, and this is due to the greater polarizability of the electron density associated with the heavier halogens (Table 19). It is of interest to note that the concept of halogen bonding involving Br/I \cdots O/N short contacts is well established. In contrast, the occurrence of interactions involving mixed halogens, namely, X \cdots F (X = Cl, Br), in the currently investigated compounds is scarce, possibly because of the reduced polarization associated with the fluorine atom itself. However, these studies are still in the nascent stages and a systematic exploration of interactions involving mixed halogens in different molecular frameworks will provide relevant insights aimed at a fundamental understanding of such interactions in the solid state. In general, the studies conducted in this article bring out the importance of halogen interactions as stabilizing motifs in the solid state.

CONCLUSIONS

The synthesis and determination of the crystal and molecular structure of a series of isomeric halogenated benzanilides provide pointers toward the existence and relative importance of strong H-bonds, weak intermolecular interactions, and halogen contacts which play an instrumental role in dictating crystal packing. Both electronic and steric factors play an important role in determining the equilibrium conformation of the molecule, and these are largely influenced by the crystal field in which such molecules reside. Such differences due to changes in functional group get manifested with concomitant changes in the nature of interactions resulting in a different crystalline symmetry and crystal packing. Although the initial formation of prenucleation aggregates is guided by intermolecular interactions regarded as an “instantaneous snapshot of crystallization”,³³ it is the crystalline symmetry which decides the final crystal structure with a minimization of the overall Gibbs free energy of formation of the solid. Thus, the magnitude of energy changes involved in such processes being small leads to the formation of polymorphs and structures having $Z' > 1$.

From a supramolecular perspective, it is indeed of interest to gain physical insights into the nature of both homo- and hetero-halogen interactions in terms of a topological characterization of chemical

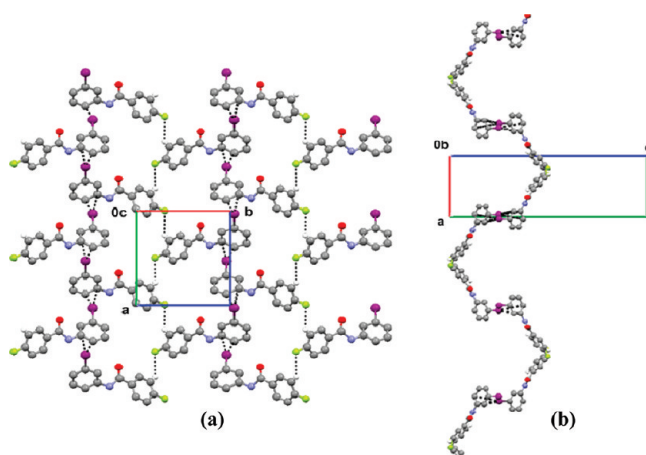


Figure 19. 4FB-3IA form (a) $\text{C}-\text{H}\cdots\text{F}$ and $\text{C}-\text{I}\cdots\pi$ parallel chains (b) helix formation through alternate $\text{C}-\text{H}\cdots\text{F}$ and $\text{C}-\text{I}\cdots\pi$ interactions.

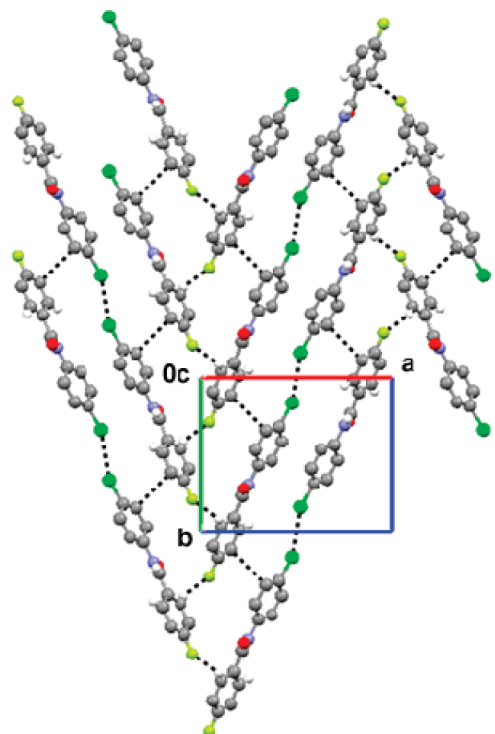


Figure 20. 4FB-4ClA forms a molecular conelike arrangement through $\text{C}-\text{H}\cdots\text{F}$, $\text{Cl}\cdots\text{Cl}$, and $\pi\cdots\pi$ interactions.

systems which contain such contacts. The one-electron properties, namely, the dipole moment, local stabilization energies, deformation density, and electrostatic potential in the $\text{C}-\text{X}/\text{Y}$ and $\text{X}\cdots\text{X}/\text{X}\cdots\text{Y}$ regions associated with such interactions is expected to provide a deeper understanding of interactions involving halogens in the solid state.

■ ASSOCIATED CONTENT

Supporting Information. ORTEP diagrams, IR spectra, experimental and simulated PXRD and NMR patterns for all the synthesized compounds, selected dihedral angles, and crystallographic information files (CIF). This material is available free of charge via the Internet at <http://pubs.acs.org>.

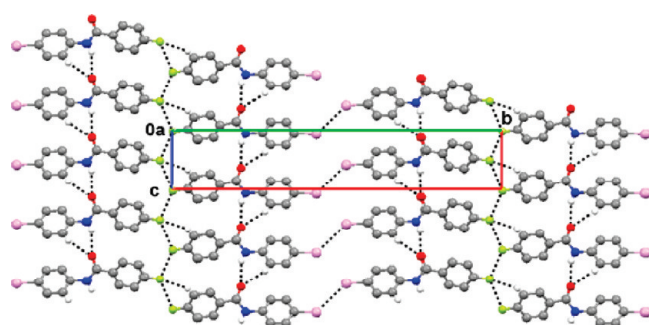


Figure 21. 4FB-4BrA form a parallel infinite chain through $\text{N}-\text{H}\cdots\text{O}$ and $\text{F}\cdots\text{F}$ interactions which are interconnected through $\text{Br}\cdots\text{Br}$ short directional contact.

Table 19. List of Interacting Mixed Halogens along with the Nature of Their Geometry

compound code	interacting halogens	type of interaction
2FA-3BrB	$\text{Br}\cdots\text{Br}$	II
2FA-4ClB	$\text{Cl}\cdots\text{Cl}$	II
2FA-4BrB	$\text{Br}\cdots\text{Br}$	II
2FA-4IB	$\text{I}\cdots\text{I}$	II
3FA-4ClB	$\text{Cl}\cdots\text{Cl}$	II
3FA-4BrB	$\text{Br}\cdots\text{Br}$	II
4FA-2ClB	$\text{F}\cdots\text{Cl}$	II
4FA-2BrB	$\text{Br}\cdots\text{F}$	II
4FA-3ClB	$\text{F}\cdots\text{F}$	I
	$\text{Cl}\cdots\text{Cl}$	II
4FA-3BrB	$\text{F}\cdots\text{F}$	I
	$\text{Br}\cdots\text{Br}$	II
4FA-4BrB	$\text{F}\cdots\text{F}$	I
	$\text{Br}\cdots\text{Br}$	II
3FB-2ClA	$\text{F}\cdots\text{F}$	I
3FB-3ClA	$\text{Br}\cdots\text{F}$	II
3FB-3ClA	$\text{Br}\cdots\text{F}$	II
4FB-2BrA	$\text{Br}\cdots\text{F}$	II
4FB-4ClA	$\text{Cl}\cdots\text{Cl}$	I
4FB-4BrA	$\text{Br}\cdots\text{Br}$	I
	$\text{F}\cdots\text{F}$	I

■ AUTHOR INFORMATION

Corresponding Author

*To whom correspondence should be addressed. D.C. Telephone: 0755-4092321. Fax: 07554092392. E-mail: dchopra@iiserbhopal.ac.in. T.N.G.R.: Telephone 080-22932796; Fax: 080-23601310; Email: ssctng@sscu.iisc.ernet.in.

■ ACKNOWLEDGMENT

We thank DST, India, for the XRD facility at IISc, and S.K.N. thanks CSIR for financial assistance. DC thanks DST-Fast Track scheme for research grant.

■ REFERENCES

- (a) Purser, S.; Moore, P. R.; Swallow, S.; Gouverneur, V. *Chem. Soc. Rev.* **2008**, 37, 320. (b) Hagmann, W. K. *J. Med. Chem.* **2008**,

- 51, 4359. (c) Jeschke, P. *Pest Manag. Sci.* **2010**, *66*, 10. (d) Hagan, D. O' J. *Fluor. Chem.* **2010**, *131*, 1071.
- (2) (a) Eustáquio, A. S.; O'Hagan, D.; Moore, B. S. *J. Nat. Prod.* **2010**, *73*, 378. (b) Wakefield, B. *Chem. Technol.*, **74**. (c) Seebach, D. *Angew. Chem. Int. Ed. Eng.* **1990**, *29*, 1320.
- (3) O'Hagan, D. *Chem. Soc. Rev.* **2008**, *37*, 308.
- (4) (a) Reichenbächer, K.; Süss, H. I.; Hulliger, J. *Chem. Soc. Rev.* **2005**, *34*, 22. (b) Schwarzer, A.; Seichter, W.; Weber, E.; Evans, H. S.; Losada, M.; Hulliger, J. *CrystEngComm* **2004**, *6*, 567. (c) Rybalova, T. V.; Bagryanskaya, I. Yu. *J. Struct. Chem.* **2009**, *50*, 741. (d) Thakur, T. S.; Kirchner, M. T.; Bläser, D.; Boese, R.; Desiraju, G. R. *CrystEngComm* **2010**, *12*, 2079.
- (5) (a) Choudhury, A. R.; Nagarajan, K.; Guru Row, T. N. *Cryst. Growth Des.* **2004**, *4*, 47. (b) Choudhury, A. R.; Guru Row, T. N. *CrystEngComm* **2006**, *8*, 265.
- (6) (a) Chopra, D.; Nagarajan, K.; Guru Row, T. N. *J. Mol. Struct.* **2008**, *888*, 70. (b) Chopra, D.; Guru Row, T. N. *CrystEngComm* **2008**, *10*, 54.
- (7) (a) Jackson, S.; Degrado, W.; Dwivedi, A.; Parthasarathy, A.; Higley, A.; Krywko, J.; Rockwell, A.; Markwalder, J.; Wells, G.; Wexler, R.; Mousa, S.; Harlow, R. *J. Am. Chem. Soc.* **1994**, *116*, 3220. (b) Capdeville, R.; Buchdunger, E.; Zimmermann, J.; Matter, A. *Nat. Rev. Drug Discovery* **2002**, *1*, 493. (c) Makino, S.; Nakanishi, E.; Tsuji, T. *Bull. Korean Chem. Soc.* **2003**, *24*, 389. (d) Zhichkin, P.; Kesicki, E.; Treiberg, J.; Bourdon, L.; Ronsheim, M.; Ooi, H. C.; White, S.; Judkins, A.; Fairfax, D. *Org. Lett.* **2007**, *9*, 1415.
- (8) (a) Bondiwell, W. E.; Chan, J. A. U.S. Patent 6515027, 2003. (b) Wickenden, A. O.; Gross, M. F.; McNaughton-Smith, G. A. U.S. Patent 6989398, 2006.
- (9) (a) Chopra, D.; Nagarajan, K.; Guru Row, T. N. *Cryst. Growth Des.* **2005**, *5*, 1035. (b) Chopra, D.; Guru Row, T. N. *Cryst. Growth Des.* **2005**, *5*, 1679. (c) Chopra, D.; Guru Row, T. N. *Cryst. Growth Des.* **2008**, *8*, 848. (d) Chopra, D.; Guru Row, T. N. *Cryst. Growth Des.* **2006**, *6*, 1267.
- (10) (a) Chopra, D.; Thiruvenkatam, V.; Guru Row, T. N. *Cryst. Growth Des.* **2006**, *6*, 843. (b) Chopra, D.; Thiruvenkatam, V.; Manjunath, S. G.; Guru Row, T. N. *Cryst. Growth Des.* **2007**, *7*, 868.
- (11) Chopra, D.; Cameron, T. S.; Ferrara, J. D.; Guru Row, T. N. *J. Phys. Chem. A* **2006**, *110*, 10465.
- (12) Li, C.; Ren, S. F.; Hou, J. L.; Yi, H. P.; Zhu, S. Z.; Jiang, X. K.; Li, Z. T. *Angew. Chem., Int. Ed. Engl.* **2005**, *44*, 5725.
- (13) (a) Zhu, Y. Y.; Yi, H. P.; Li, C.; Jiang, X. K.; Li, Z. T. *Cryst. Growth Des.* **2008**, *8*, 1294. (b) Zhu, Y. Y.; Jiang, L.; Li, Z. T. *CrystEngComm* **2009**, *11*, 235.
- (14) (a) Du, P.; Jiang, X. K.; Li, Z. T. *Tet. Lett.* **2009**, *50*, 316. (b) Moorthy, J. N.; Natarajan, R.; Mal, P.; Venugopalan, P. *J. Am. Chem. Soc.* **2002**, *124*, 6530.
- (15) (a) Pedireddi, V. R.; Reddy, S. D.; Goud, B. S.; Craig, D. C.; Rae, A. D.; Desiraju, G. R. *J. Chem. Soc. Perkin Trans. 2* **1994**, 2353. (b) Saraogi, I.; Vijay, V. G.; Das, S.; Sekar, K.; Guru Row, T. N. *Crystalogr. Eng.* **2003**, *6*, 69. (c) Prasanna, M. D.; Guru Row, T. N. *Crystalogr. Eng.* **2000**, *3*, 135.
- (16) (a) Hassel, O. *Science* **1970**, *170*, 497. (b) Ramasubbu, N.; Parthasarathy, R.; Rust, M. P. *J. Am. Chem. Soc.* **1986**, *108*, 4308. (c) Desiraju, G. R.; Parthasarathy, R. *J. Am. Chem. Soc.* **1989**, *111*, 8725. (d) Reddy, C. M.; Kirschner, M. T.; Gundakaram, R. C.; Padmanabhan, K. A.; Desiraju, G. R. *Chem.—Eur. J.* **2006**, *12*, 2222. (e) Samai, S.; Biradha, K. *CrystEngComm* **2009**, *11*, 482. (f) Nyburg, S. C.; Wong-Ng, W. *Inorg. Chem.* **1979**, *18*, 2790. (g) Williams, D. E. *J. Chem. Phys.* **1967**, *47*, 4680. (h) Bui, T. T. T.; Dahaoui, S.; Lecomte, C.; Desiraju, G. R.; Espinosa, E. *Angew. Chem., Int. Ed.* **2009**, *48*, 3838. (i) Desiraju, G. R.; Parthasarathy, R. *J. Am. Chem. Soc.* **1989**, *111*, 8725. (j) Bosch, E.; Barnes, C. L. *Cryst. Growth Des.* **2002**, *2*, 299. (k) Saha, B. K.; Nangia, A.; Nicoud, J. F. *Cryst. Growth Des.* **2006**, *6*, 1278. (l) Pigge, F. C.; Vangala, V. R.; Swenson, D. C. *Chem. Commun.* **2006**, 2123. (m) Anthony, A.; Desiraju, G. R.; Kuduva, S. S.; Madhavi, N. N. L.; Nangia, A.; Thaimattam, R.; Thalladi, V. R. *Cryst. Eng.* **1998**, *1*, 1. (n) Jetti, R. K. R.; Xue, F.; Mak, T. C. W.; Nangia, A. *Crystalogr. Eng.* **1999**, *2*, 215.
- (17) (a) Gowda, B. T.; Sowmya, B. P.; Kozisek, J.; Tokarcik, M.; Fuess, H. *Acta Crystallogr.* **2007**, *E63*, o2906. (b) Gowda, B. T.; Sowmya, B. P.; Tokarcik, M.; Kozisek, J.; Fuess, H. *Acta Crystallogr.* **2007**, *E63*, o3326. (c) Gowda, B. T.; Sowmya, B. P.; Tokarcik, M.; Kozisek, J.; Fuess, H. *Acta Crystallogr.* **2007**, *E63*, o3365. (d) Gowda, B. T.; Tokarcik, M.; Kozisek, J.; Sowmya, B. P.; Fuess, H. *Acta Crystallogr.* **2008**, *E64*, o462. (e) Gowda, B. T.; Sowmya, B. P.; Kozisek, J.; Tokarcik, M.; Fuess, H. *Acta Crystallogr.* **2007**, *E63*, o2906. (f) Gowda, B. T.; Foro, S.; Sowmya, B. P.; Fuess, H. *Acta Crystallogr.* **2007**, *E63*, o3789. (g) Gowda, B. T.; Tokarcik, M.; Kozisek, J.; Sowmya, B. P.; Fuess, H. *Acta Crystallogr.* **2008**, *E64*, o540. (h) Gowda, B. T.; Tokarcik, M.; Kozisek, J.; Sowmya, B. P.; Fuess, H. *Acta Crystallogr.* **2008**, *E64*, o769. (i) Gowda, B. T.; Foro, S.; Sowmya, B. P.; Fuess, H. *Acta Crystallogr.* **2008**, *E64*, o861. (j) Gowda, B. T.; Foro, S.; Sowmya, B. P.; Fuess, H. *Acta Crystallogr.* **2008**, *E64*, o949. (k) Gowda, B. T.; Tokarcik, M.; Kozisek, J.; Sowmya, B. P.; Fuess, H. *Acta Crystallogr.* **2008**, *E64*, o950. (l) Gowda, B. T.; Foro, S.; Sowmya, B. P.; Fuess, H. *Acta Crystallogr.* **2008**, *E64*, o1243. (m) Gowda, B. T.; Foro, S.; Sowmya, B. P.; Fuess, H. *Acta Crystallogr.* **2008**, *E64*, o1294. (n) Gowda, B. T.; Foro, S.; Sowmya, B. P.; Fuess, H. *Acta Crystallogr.* **2008**, *E64*, o1300. (o) Gowda, B. T.; Foro, S.; Sowmya, B. P.; Fuess, H. *Acta Crystallogr.* **2008**, *E64*, o1342. (p) Gowda, B. T.; Foro, S.; Sowmya, B. P.; Fuess, H. *Acta Crystallogr.* **2008**, *E64*, o1421. (q) Gowda, B. T.; Tokarcik, M.; Kozisek, J.; Sowmya, B. P.; Fuess, H. *Acta Crystallogr.* **2008**, *E64*, o1493. (r) Gowda, B. T.; Tokarcik, M.; Kozisek, J.; Sowmya, B. P.; Fuess, H. *Acta Crystallogr.* **2008**, *E64*, o1365. (s) Saeed, A.; Khera, R. A.; Gotoh, K.; Ishida, H. *Acta Crystallogr.* **2008**, *E64*, o1934. (t) Saeed, A.; Khera, R. A.; Abbas, N.; Simpson, J.; Stanley, R. G. *Acta Crystallogr.* **2008**, *E64*, o1976. (u) Gowda, B. T.; Foro, S.; Sowmya, B. P.; Fuess, H. *Acta Crystallogr.* **2009**, *E65*, o444. (v) Saeed, A.; Khera, R. A.; Arfan, M.; Simpson, J.; Stanley, R. G. *Acta Crystallogr.* **2009**, *E65*, o802. (w) Saeed, A.; Khera, R. A.; Ameen, S.; Simpson, J.; Stanley, R. G. *Acta Crystallogr.* **2009**, *E65*, o201. (x) Tokarcik, M.; Gowda, B. T.; Kozisek, J.; Sowmya, B. P.; Fuess, H. *Acta Crystallogr.* **2009**, *E65*, o1637. (y) Tan, Z.; Bing, Y.; Fang, S.; Kai, Z.; Yan, Y. *Acta Crystallogr.* **2009**, *E65*, o1757.
- (18) Grabowski, S. J.; Sadlej, A. J.; Sokalski, W. A.; Leszczynski *J. Chem. Phys.* **2006**, *127*, 151.
- (19) Serezhkin, V. V.; Prokava, M. A.; Pushkin, D. V.; Serezhkina, L. B. *Russ. J. Inorg. Chem.* **2009**, *54*, 1251.
- (20) Nayak, S. K.; Reddy, M. K.; Guru Row, T. N. *Private Communication*, 2010.
- (21) Chopra, D.; Guru Row, T. N. *J. Mol. Struct.* **2005**, *733*, 133.
- (22) SMART (V 5.628), SAINT (V 6.45a), SADABS, XPREP, SHELLXTL; Bruker AXS Inc: Madison, WI, 2004.
- (23) CrystAlis CCD and CrystAlis RED, Version 1.171.33.31; Oxford Diffraction Ltd: Abingdon, Oxfordshire, England, 2009.
- (24) Sheldrick, G. M. *Acta Crystallogr.* **2008**, *A64*, 112.
- (25) Farrugia, L. J. *WinGX* (V 1.70.01). *J. Appl. Crystallogr.* **1999**, *32*, 837.
- (26) (a) Farrugia, L. J. *J. Appl. Crystallogr.* **1997**, *30*, S65. (b) Burnett, M. N.; Johnson, C. K. Report ORNL-6895; Oak Ridge National Laboratory: Oak Ridge Tennessee, 1996.
- (27) Macrae, C. F.; Bruno, I. J.; Chisholm, J. A.; Edgington, P. R.; McCabe, P.; Pidcock, E.; Rodriguez-Monge, L.; Taylor, R.; Streck, J.; Wood, P. A. *J. Appl. Crystallogr.* **2008**, *41*, 466; www.ccdc.cam.ac.uk/mercury.
- (28) Nardelli, M. J. *J. Appl. Crystallogr.* **1995**, *28*, 569.
- (29) Spek, A. L. *Acta Crystallogr.* **1990**, *A46*, c34.
- (30) (a) Kashino, S.; Ito, K.; Haisa, M. *Bull. Chem. Soc. Jpn.* **1979**, *52*, 365. (b) Bowes, K. F.; Glidewell, C.; Low, J. N.; Skakle, J. M. S.; Wardell, J. S. *Acta Crystallogr.* **2003**, *C59*, o1.
- (31) Chopra, D.; Guru Row, T. N. *CrystEngComm* **2008**, *10*, 54.
- (32) K'alm'an, A. *Acta Crystallogr.* **2005**, *B61*, 536.
- (33) Das, D.; Banerjee, R.; Mondal, R.; Howard, J. A. K.; Boese, R.; Desiraju, G. R. *Chem. Commun.* **2006**, 555.
- (34) Manjunatha Reddy, G. N.; Vasantha Kumar, M. V.; Guru Row, T. N.; Suryaprakash, N. *Phys. Chem. Chem. Phys.* **2010**, *12*, 13232.
- (35) Dance, I. *New J. Chem.* **2003**, *27*, 22.
- (36) Poglani, L. *New J. Chem.* **2003**, *27*, 919.
- (37) Pedireddi, V. R.; Reddy, D. S.; Goud, B. S.; Craig, D. C.; Rae, A. D.; Desiraju, G. R. *J. Chem. Soc. Perkin Trans. 2* **1994**, 2353.
- (38) Saha, B. K.; Nangia, A.; Nicoud, J.-F. *Cryst. Growth Des.* **2006**, *6*, 1278.